C3PO, a ray-tracing code for arbitrary axisymmetric magnetic equilibrium

Yves Peysson and Joan Decker

09/01/2008

Contents

1 Introduction

In order to calculate power and current deposition from RF waves in plasmas, it is necessary to determine the wave characteristics inside the plasma. In a quasi-stationary plasma where the equilibrium varies on a scale that is much larger than the wavelength, it is possible to calculate the wave propagation from antenna or mirror conditions and equilibrium properties using the ray-tracing techniques. This method has been used extensively for calculating lower-hybrid and electron cyclotron wave propagation [1, 2, 3, 4].

Many ray tracing codes in axisymmetric toroidal plasmas use the toroidal coordinates (R, Z, ϕ) which are attractive because of the simplicity of implementing the equations in this system [5, 6, 7, 4]. In this work we use the flux coordinates (ρ, θ, ϕ) instead. While the equations in this system require somewhat more complicated metric coefficients, there are several advantages to this choice: first, any equilibrium property that is a flux function, such as the density and temperature - or more generally the distribution function

-, depends upon ρ only; second, the periodicity of the coordinate θ allows the use of Fourier series that are particularly useful for accurate interpolation and the calculation of derivatives up to second order; third, this system is used by a variety of codes that are coupled to the ray-tracing solver, such as equilibrium codes (HELENA) and Fokker-Planck solvers (LUKE) [8, 9]. Using the same system in the ray-tracing code saves any coordinates conversions and grid interpolations which introduce numerical errors.

The new ray-tracing code developed here is designed for arbitrary wave frequencies (including the lower hybrid and electron cyclotron frequency ranges), provided the WKB approximation is valid. The structure of the code allows to choose from several dielectric tensor types: cold plasma, "warm" plasma [10], and kinetic plasma in the non-, weakly-, or fully relativistic regime. In addition to ray trajectories, the code calculates waves properties of interest for heating and current drive calculations such as the polarization, energy flow and linear absorption.

Based on a standard 6^{th} order Runge-Kutta differential scheme [11], the ray-tracing code uses a spline-Fourier expansion for equilibrium interpolation, which results in fast yet accurate calculations. The code is distributed as a mexfile[1] written in C language. It is benchmarked extensively for various types of waves against both existing codes and analytical models. In Sec.2, the linear wave theory in an infinite uniform medium is presented. Ray-tracing in slowly varying plasma is derived in Sec.3. The curvilinear canonical flux coordinates in an axisymmetric toroidal plasma are introduced in Sec.4. In Sec.5 numerical methods are presented. A conclusion is given in Sec.6. The Appendix includes some properties of the coordinate system (A), explicit expressions for the dispersion relations and some derivatives (B), the cold and hot plasma dielectric tensors (C,D), and the benchmarking results (E).

2 Linear wave theory in an infinite uniform plasma

2.1 Maxwell's equations

Electromagnetic fields are generated by charge and current densities according to Maxwell's equations

$$\begin{aligned} \nabla \cdot \mathbf{E} &= \frac{\rho}{\varepsilon_0} \\ \nabla \cdot \mathbf{B} &= 0 \\ \nabla \times \mathbf{E} &= -\frac{\partial \mathbf{B}}{\partial t} \\ \nabla \times \mathbf{B} &= \mu_0 \mathbf{J} + \varepsilon_0 \mu_0 \frac{\partial \mathbf{E}}{\partial t} \end{aligned} \tag{1}$$

where $\mathbf{E}(\mathbf{X}, t)$ and $\mathbf{B}(\mathbf{X}, t)$ are the electric and magnetic fields, $\rho(\mathbf{X}, t)$ and $\mathbf{J}(\mathbf{X}, t)$ are the charge and current densities. Here, $\mathbf{X}$ is the vector position, and t is the time. The continuity equation - or charge conservation - relating the charge density $\rho(\mathbf{X}, t)$ to the current density $\mathbf{J}(\mathbf{X}, t)$ is obtained from (1)

$$\frac{\partial \rho}{\partial t} + \nabla \cdot \mathbf{J} = 0 \tag{2}$$

[1]The code runs in the MatLab 7 programming environment.

2.2 Constitutive relation

Maxwell equations (1) are a closed system only if the charge and the current densities are known. In a plasma $\rho(\mathbf{X},t)$ and $\mathbf{J}(\mathbf{X},t)$ are functions of $\mathbf{E}(\mathbf{X},t)$ and $\mathbf{B}(\mathbf{X},t)$. The expression of $\mathbf{J}(\mathbf{X},t)$ as a function of $\mathbf{E}(\mathbf{X},t)$ is called the constitutive relation. For linearized fields, this relation can be expressed in general as

$$\mathbf{J}(\mathbf{X},t) = \iiint d^3\mathbf{X}' \int dt' \, \mathbb{S}(\mathbf{X},\mathbf{X}',t,t') \cdot \mathbf{E}(\mathbf{X}',t') \tag{3}$$

where $\mathbb{S}(\mathbf{X},\mathbf{X}',t,t')$ is the conductivity tensor, which depends upon the plasma equilibrium.

2.3 Fourier transform

In a infinite plasma with an homogeneous constant equilibrium that is invariant by translation in space and time, the conductivity tensor is only a function of the relative distance in space and time, and Eq. 3 may be rewritten as a convolution

$$\mathbf{J}(\mathbf{X},t) = \iiint d^3\mathbf{X}' \int dt' \, \mathbb{S}(\mathbf{X}-\mathbf{X}',t-t') \cdot \mathbf{E}(\mathbf{X}',t') \tag{4}$$

Applying the Fourier transform to the fields yields

$$\begin{aligned} \mathbf{E}(\mathbf{X},t) &= \int d\omega \iiint d^3\mathbf{k} \, \mathbf{E}_\mathbf{k}(\mathbf{k},\omega) \, e^{i(\mathbf{k}\cdot\mathbf{X}-\omega t)} \\ \mathbf{J}(\mathbf{X},t) &= \int d\omega \iiint d^3\mathbf{k} \, \mathbf{J}_\mathbf{k}(\mathbf{k},\omega) \, e^{i(\mathbf{k}\cdot\mathbf{X}-\omega t)} \end{aligned} \tag{5}$$

with the reverse relations

$$\begin{aligned} \mathbf{E}_\mathbf{k}(\mathbf{k},\omega) &= \frac{1}{(2\pi)^4} \iiint d^3\mathbf{X} \int dt \, \mathbf{E}(\mathbf{X},t) \, e^{-i(\mathbf{k}\cdot\mathbf{X}-\omega t)} \\ \mathbf{J}_\mathbf{k}(\mathbf{k},\omega) &= \frac{1}{(2\pi)^4} \iiint d^3\mathbf{X} \int dt \, \mathbf{J}(\mathbf{X},t) \, e^{-i(\mathbf{k}\cdot\mathbf{X}-\omega t)} \end{aligned} \tag{6}$$

such that (4) becomes

$$\mathbf{J}_\mathbf{k}(\mathbf{k},\omega) = \mathbb{S}(\mathbf{k},\omega) \cdot \mathbf{E}_\mathbf{k}(\mathbf{k},\omega) \tag{7}$$

Similarly, applying the Fourier transform to the Maxwell's equations gives

$$\begin{aligned} i\mathbf{k}\cdot\mathbf{E}_\mathbf{k} &= \frac{\rho_\mathbf{k}}{\varepsilon_0} \\ i\mathbf{k}\cdot\mathbf{B}_\mathbf{k} &= 0 \\ i\mathbf{k}\times\mathbf{E}_\mathbf{k} &= i\omega\mathbf{B}_\mathbf{k} \\ i\mathbf{k}\times\mathbf{B}_\mathbf{k} &= \mu_0\mathbf{J}_\mathbf{k} - \varepsilon_0\mu_0 i\omega\mathbf{E}_\mathbf{k} \end{aligned} \tag{8}$$

2.4 Linear wave equation

Combining the last two equations in (8) with (7) leads to the linear wave equation

$$\mathbf{k}\times\mathbf{k}\times\mathbf{E}_\mathbf{k} + \frac{\omega^2}{c^2}\mathbb{K}(\mathbf{k},\omega)\cdot\mathbf{E}_\mathbf{k} = 0 \tag{9}$$

where

$$\mathbb{K}(\mathbf{k},\omega) = \mathbb{I} + \mathbb{X}(\mathbf{k},\omega) \tag{10}$$

is the permittivity tensor,

$$\mathbb{X}(\mathbf{k},\omega) = \frac{i}{\varepsilon_0 \omega}\mathbb{S}(\mathbf{k},\omega) \tag{11}$$

is the susceptibility tensor and $\mathbb{I}$ is the unit tensor.

Introducing the index of refraction

$$\mathbf{N} \equiv \frac{c}{\omega}\mathbf{k} \tag{12}$$

the wave equation becomes

$$\mathbf{N} \times \mathbf{N} \times \mathbf{E}_\mathbf{k} + \mathbb{K}(\mathbf{N},\omega) \cdot \mathbf{E}_\mathbf{k} = 0 \tag{13}$$

or equivalently

$$\mathbb{D} \cdot \mathbf{E}_\mathbf{k} = 0 \tag{14}$$

where $\mathbb{D}(\mathbf{N},\omega)$

$$\mathbb{D} = \mathbf{NN} - N^2\mathbb{I} + \mathbb{K}(\mathbf{N},\omega) \tag{15}$$

is the dispersion tensor. The susceptibility $\mathbb{X}$ is the sum of contributions from all species

$$\mathbb{X} = \sum_s \mathbb{X}^s \tag{16}$$

In the case where the distribution function of the species s is a Maxwellian, $\mathbb{X}^s$ depends upon the following non-dimensional parameters : the refractive index $\mathbf{N}$, the thermal velocity normalized to the speed of light $\beta_{Ts} = v_{Ts}/c$ where $v_{Ts} = \sqrt{kT_s/m_s}$, and the ratios $\overline{\omega}_{ps} = \omega_{ps}/\omega$ and $\overline{\omega}_{cs} = \omega_{cs}/\omega$ of the plasma frequency $\omega_{ps} = \sqrt{q_s^2 n_s/\varepsilon_0 m_s}$ and the cyclotron frequency $\omega_{cs} = q_s B_0/m_s$ to the wave frequency ω. Therefore the dispersion tensor may be expressed in the general form

$$\mathbb{D} = \mathbf{NN} - \mathbf{N}^2\mathbb{I} + \mathbb{K}(\mathbf{N}, \beta_{Ts}, \overline{\omega}_{ps}, \overline{\omega}_{cs}) \tag{17}$$

2.5 Dispersion relation

In order to obtain non-trivial solutions to the Eq. 14, the determinant of the dispersion tensor must be zero,

$$\mathcal{D}(\mathbf{N}, \beta_{Ts}, \overline{\omega}_{ps}, \overline{\omega}_{cs}) \equiv \det \mathbb{D}(\mathbf{N}, \beta_{Ts}, \overline{\omega}_{ps}, \overline{\omega}_{cs}) = 0 \tag{18}$$

which defines the dispersion relation. This relation gives the local electromagnetic eigenmodes that can be excited independently in the homogenous plasma. By cylindrical symmetry about the direction of the magnetic field $\hat{\mathbf{b}} = \mathbf{B}_0/B_0$, $\mathcal{D}$ depends only upon the components of $\mathbf{N}$ parallel and perpendicular to the magnetic field, defined respectively as $N_\parallel = \mathbf{N}\cdot\hat{\mathbf{b}}$ and $N_\perp = \left\|\mathbf{N} \times \hat{\mathbf{b}}\right\|$. Thus, the dispersion relation (18) can be solved for either $\omega\left(N_\parallel, N_\perp\right)$, $N_\parallel(\omega, N_\perp)$ or $N_\perp\left(\omega, N_\parallel\right)$. The polarization of any eigenmode resulting from equation (18) is determined by the corresponding eigenvector of the wave equation (14).

Explicit expressions of the dispersion relation are given in Appendix A1.

2.6 Weak damping approximation

Assuming that ω and $N_\parallel$ are given real quantities, (18) generally leads to a complex $N_\perp = N_{\perp r} + iN_{\perp i}$. Meanwhile, the dispersion tensor $\mathbb{D}$ can be generally decomposed as $\mathbb{D} = \mathbb{D}^{\mathrm{H}} + i\mathbb{D}^{\mathrm{A}}$ where $\mathbb{D}^{\mathrm{H}} = (\mathbb{D} + \mathbb{D}^\dagger)/2$ and $\mathbb{D}^{\mathrm{A}} = (\mathbb{D} - \mathbb{D}^\dagger)/2i$ are the hermitian and antihermitian parts of $\mathbb{D}$, respectively. In this work, the weak damping approximation is considered, which is valid if $|D^{\mathrm{A}}_{ij}| \ll |D^{\mathrm{H}}_{ij}|$. In that case, it can be shown [12] that $|N_{\perp i}| \ll |N_{\perp r}|$ and $N_{\perp r}$ can be determined from solving the approximate wave equation

$$\mathbb{D}^{\mathrm{H}}\left(N_{\perp r}\right) \cdot \mathbf{E}_{\mathbf{k}} = 0 \tag{19}$$

with dispersion relation

$$\mathcal{D}^{\mathrm{H}}\left(N_\parallel, N_{\perp r}, \beta_{Ts}, \overline{\omega}_{ps}, \overline{\omega}_{cs}\right) \equiv \det \mathbb{D}^{\mathrm{H}}\left(N_\parallel, N_{\perp r}, \beta_{Ts}, \overline{\omega}_{ps}, \overline{\omega}_{cs}\right) = 0 \tag{20}$$

In this approximation, the time-averaged densities of energy flow $\mathbf{S}$ and dissipated power P can be obtained from

$$\begin{aligned} \mathbf{S} &= -\frac{\varepsilon_0 c}{4}\frac{\partial}{\partial \mathbf{N}}\left(\mathbf{E}^*_{\mathbf{k}} \cdot \mathbb{D}^{\mathrm{H}} \cdot \mathbf{E}_{\mathbf{k}}\right) \\ P &= \frac{\varepsilon_0 \omega}{2}\mathbf{E}^*_{\mathbf{k}} \cdot \mathbb{D}^{\mathrm{A}} \cdot \mathbf{E}_{\mathbf{k}} \end{aligned} \tag{21}$$

Note that the imaginary part of the wave vector can be calculated using

$$N_{\perp i} = \frac{c}{2\omega}\frac{P}{S_\perp} \tag{22}$$

which yields the ray damping. From here on in this paper, $\mathbf{k}$ and $\mathbf{N}$ will refer to the zero-order, real solution of (20), and the dispersion relation $\mathcal{D}$ to the hermitian part $\mathcal{D}^{\mathrm{H}}$.

3 Ray tracing in a slowly varying plasma

3.1 WKB Approximation

In a slightly nonuniform plasma where

$$\|\mathbf{k}\| \gg \frac{\|\nabla \beta_{Ts}\|}{\beta_{Ts}}, \frac{\|\nabla \overline{\omega}_{ps}\|}{\overline{\omega}_{ps}}, \frac{\|\nabla \overline{\omega}_{cs}\|}{|\overline{\omega}_{cs}|} \tag{23}$$

and the wave characteristics also vary slowly

$$\|\mathbf{k}\|^2 \gg \|\nabla k\| \tag{24}$$

the wave equation (19) and dispersion relation (20) are still be satisfied locally, under the WKB approximation. The wave vector $\mathbf{k}$ is then a slowly varying function of space and $\mathbf{k}\left(\mathbf{X}\right)$ can be determined using ray-tracing techniques.

3.2 Ray equations

Ray equations in a plasma slowly varying in space and time are defined by the condition (20) $\mathcal{D}\left(\mathbf{X}, t, \mathbf{k}, \omega\right) = 0$ along the ray trajectory. Therefore, at all points along the ray trajectory, the condition

$$\delta\mathcal{D} = \frac{\partial \mathcal{D}}{\partial \mathbf{X}} \cdot \delta\mathbf{X} + \frac{\partial \mathcal{D}}{\partial t}\delta t + \frac{\partial \mathcal{D}}{\partial \mathbf{k}} \cdot \delta\mathbf{k} + \frac{\partial \mathcal{D}}{\partial \omega}\delta\omega = 0 \tag{25}$$

must be satisfied. Let define τ a dimensionless parameter, which is a measure of distance along the trajectory. Then (25) can be rewritten as

$$\delta\mathcal{D} = \frac{\partial\mathcal{D}}{\partial\mathbf{X}} \cdot \dot{\mathbf{X}}\delta\tau + \frac{\partial\mathcal{D}}{\partial t}\dot{t}\delta\tau + \frac{\partial\mathcal{D}}{\partial\mathbf{k}} \cdot \dot{\mathbf{k}}\delta\tau + \frac{\partial\mathcal{D}}{\partial\omega}\dot{\omega}\delta\tau = 0 \tag{26}$$

where $\dot{\mathbf{X}} = d\mathbf{X}/d\tau$, $\dot{\mathbf{k}} = d\mathbf{k}/d\tau$, $\dot{t} = dt/d\tau$ and $\dot{\omega} = d\omega/d\tau$. The wave vector $\mathbf{k}$ is expressed in coordinates that are canonically conjugate to those of the position vector $\mathbf{X}$

$$\{X_i, k_j\} = \delta_{ij} \tag{27}$$

where $\{\ldots\}$ is Poisson bracket, δ_{ij} is the Kronecker delta symbol, X_i and k_j are the coordinate of $\mathbf{X}$ and $\mathbf{k}$ respectively. The frequency ω and the time t being also canonically conjugate, the relations

$$\begin{aligned} \frac{d\mathbf{X}}{d\tau} &= \frac{\partial\mathcal{D}}{\partial\mathbf{k}} \\ \frac{d\mathbf{k}}{d\tau} &= -\frac{\partial\mathcal{D}}{\partial\mathbf{X}} \\ \frac{dt}{d\tau} &= -\frac{\partial\mathcal{D}}{\partial\omega} \\ \frac{d\omega}{d\tau} &= \frac{\partial\mathcal{D}}{\partial t} \end{aligned} \tag{28}$$

result from the Hamiltonian nature of $\mathcal{D}$, and Eq. 26 is automatically satisfied. These four equations are therefore the ray equations. From the first and the third equations,

$$\frac{d\mathbf{X}}{dt} = -\frac{\partial\mathcal{D}}{\partial\mathbf{k}} \Big/ \frac{\partial\mathcal{D}}{\partial\omega} = \frac{\partial\omega}{\partial\mathbf{k}} = \mathbf{v}_g \tag{29}$$

meaning that the ray is directed along the group velocity $\mathbf{v}_g$ and thus indicates the direction of energy flow since $\mathbf{v}_g \| \mathbf{S}$ [13]. In a constant plasma $\partial\mathcal{D}/\partial t = 0$ and ω is a constant of the ray dynamics. The time t is considered as the evolution parameter of the ray and the two remaining equations are

$$\begin{aligned} \frac{d\mathbf{X}}{dt} &= -\frac{\partial\mathcal{D}}{\partial\mathbf{k}} \Big/ \frac{\partial\mathcal{D}}{\partial\omega} \\ \frac{d\mathbf{k}}{dt} &= \frac{\partial\mathcal{D}}{\partial\mathbf{X}} \Big/ \frac{\partial\mathcal{D}}{\partial\omega} \end{aligned} \tag{30}$$

which are the usual forms found in the literature. However, one may also keep the simple form

$$\begin{aligned} \frac{d\mathbf{X}}{d\tau} &= \frac{\partial\mathcal{D}}{\partial\mathbf{k}} \\ \frac{d\mathbf{k}}{d\tau} &= -\frac{\partial\mathcal{D}}{\partial\mathbf{X}} \end{aligned} \tag{31}$$

if the determination of the group velocity from $\partial\mathcal{D}/\partial\omega$ is not required. This reduces the number of derivative to calculate.

We define $\mathbf{Y}$ the 8-dimension vector that represents the phase-space coordinates

$$\mathbf{Y} = \begin{pmatrix} \mathbf{X} \\ \mathbf{k} \\ t \\ \omega \end{pmatrix} \tag{32}$$

The ray equations (30-31) require to evaluate the derivatives of the dispersion relation (20) with respect to the coordinates of $\mathbf{Y}$, explicitly

$$\frac{\partial N_{\parallel}}{\partial \mathbf{Y}}; \quad \frac{\partial N_{\perp}}{\partial \mathbf{Y}}; \quad \frac{\partial X_{ij}^{s}}{\partial \mathbf{Y}} \tag{33}$$

Since $\mathbb{X}^s = \mathbb{X}^s \left(N_{\perp}, N_{\parallel}, \beta_{Ts}, \overline{\omega}_{ps}, \overline{\omega}_{cs}\right)$,

$$\begin{aligned} \frac{\partial X_{ij}^{s}}{\partial \mathbf{Y}} = & \frac{\partial X_{ij}^{s}}{\partial N_{\perp}} \frac{\partial N_{\perp}}{\partial \mathbf{Y}} + \frac{\partial X_{ij}^{s}}{\partial N_{\parallel}} \frac{\partial N_{\parallel}}{\partial \mathbf{Y}} \\ & + \frac{\partial X_{ij}^{s}}{\partial \beta_{Ts}} \frac{\partial \beta_{Ts}}{\partial \mathbf{Y}} + \frac{\partial X_{ij}^{s}}{\partial \overline{\omega}_{ps}} \frac{\partial \overline{\omega}_{ps}}{\partial \mathbf{Y}} + \frac{\partial X_{ij}^{s}}{\partial \overline{\omega}_{cs}} \frac{\partial \overline{\omega}_{cs}}{\partial \mathbf{Y}} \end{aligned} \tag{34}$$

In this equation the derivatives of the susceptibility tensor depend upon the plasma dispersion model (i.e. cold, kinetic, etc) while the derivatives with respect to $\mathbf{Y}$ are function of the equilibrium and the coordinate system.

4 Canonical coordinates in an axisymmetric toroidal plasma

4.1 Flux coordinate system

In an axisymmetric toroidal plasma we define the coordinate system (ρ, θ, ϕ) where θ is the poloidal angle measured counterclockwise from the horizontal outboard midplane, ϕ is the toroidal angle measured clockwise from the top, and ρ is a radial coordinate that varies between 0 on the axis and 1 at the plasma edge. The coordinate $\rho = \rho(\psi)$ must be a flux function, i.e. a monotonic function of the poloidal magnetic flux coordinate ψ defined by the following expression of the magnetic field [9]

$$\mathbf{B} = I(\psi) \nabla\phi + \nabla\phi \times \nabla\psi \tag{35}$$

which can be rewritten as

$$\mathbf{B} = \sigma_B B_T \hat{\phi} + \sigma_I B_P \hat{\mathbf{s}} \tag{36}$$

where σ_B is the sign of B_ϕ and σ_I is the sign of I_ϕ. $B_T = |I(\psi)|/R$ and $B_P = \|\nabla\psi\|/R$ are definite positive and $\hat{\mathbf{s}} = \hat{\phi} \times \hat{\rho}$ with $\nabla\rho = \|\nabla\rho\| \hat{\rho}$ such that $\hat{\mathbf{s}}$ is orientated counterclockwise in the poloidal plane.

In the (ρ, θ, ϕ) coordinate system the covariant coordinates of the wave vector $\mathbf{k}$ are

$$k_i = (k_\rho, m, n) \tag{37}$$

The Poisson matrix of canonically conjugate $\mathbf{X}$ and $\mathbf{k}$ is

$$\{\mathbf{X}, \mathbf{k}\} = \frac{\partial \mathbf{X}}{\partial \mathbf{X}} \cdot \frac{\partial \mathbf{k}}{\partial \mathbf{k}} - \frac{\partial \mathbf{X}}{\partial \mathbf{k}} \cdot \frac{\partial \mathbf{k}}{\partial \mathbf{X}} = \mathbb{I} \tag{38}$$

4.2 Ray equations

In the canonically conjugate systems (ρ, θ, ϕ) and (k_ρ, m, n) the ray equations becomes

$$\begin{aligned}
\frac{d\rho}{dt} &= -\frac{\partial \mathcal{D}}{\partial k_\rho} \Big/ \frac{\partial \mathcal{D}}{\partial \omega} \\
\frac{d\theta}{dt} &= -\frac{\partial \mathcal{D}}{\partial m} \Big/ \frac{\partial \mathcal{D}}{\partial \omega} \\
\frac{d\phi}{dt} &= -\frac{\partial \mathcal{D}}{\partial n} \Big/ \frac{\partial \mathcal{D}}{\partial \omega}
\end{aligned} \tag{39}$$

and

$$\begin{aligned}
\frac{dk_\rho}{dt} &= \frac{\partial \mathcal{D}}{\partial \rho} \Big/ \frac{\partial \mathcal{D}}{\partial \omega} \\
\frac{dm}{dt} &= \frac{\partial \mathcal{D}}{\partial \theta} \Big/ \frac{\partial \mathcal{D}}{\partial \omega} \\
\frac{dn}{dt} &= \frac{\partial \mathcal{D}}{\partial \phi} \Big/ \frac{\partial \mathcal{D}}{\partial \omega}
\end{aligned} \tag{40}$$

For an axisymmetric magnetic configuration, $\partial \mathcal{D}/\partial \phi = 0$ such that n is an invariant. Therefore, only the first five equations need to be solved. The value of n is determined from launching conditions.

4.3 Parallel index of refraction

The parallel index of refraction is defined as

$$k_\parallel = \frac{1}{B}\mathbf{k} \cdot \mathbf{B} = \frac{1}{B} k_i B^j \tag{41}$$

Here B^j are the contravariant coordinates of $\mathbf{B}$, given by

$$B^j = \mathbf{B} \cdot \mathbf{e}^j \tag{42}$$

where

$$\mathbf{e}^j = \left(\|\nabla \rho\| \, \hat{\rho}, \frac{\hat{\theta}}{r}, \frac{\hat{\phi}}{R} \right) \tag{43}$$

such that the contravariant coordinates of $\mathbf{B}$ are

$$B^j = \left(0, \frac{\sigma_I B_P}{r} \cos\alpha, \frac{\sigma_B B_T}{R} \right) \tag{44}$$

where α is the angle between $\widehat{\rho}$ to $\widehat{\mathbf{r}}$ such that

$$\begin{aligned}
\hat{\rho} \cdot \hat{\mathbf{r}} &= \cos\alpha \\
\hat{\rho} \cdot \hat{\theta} &= -\sin\alpha \\
\hat{\mathbf{s}} \cdot \hat{\mathbf{r}} &= \sin\alpha \\
\hat{\mathbf{s}} \cdot \hat{\theta} &= \cos\alpha
\end{aligned} \tag{45}$$

Because $\hat{\rho}$ is orientated outward we have $-\pi/2 < \alpha < \pi/2$. Then (41) yields

$$\boxed{k_{\parallel} = \sigma_I \cos\alpha P \frac{m}{r} + \sigma_B T \frac{n}{R}} \tag{46}$$

where $P = \dfrac{B_P}{B}$ and $T = \dfrac{B_T}{B}$.

4.4 Perpendicular index of refraction

The squared norm of $\mathbf{k}$ is given by

$$k^2 = g^{ij} k_i k_j \tag{47}$$

which is explicitly

$$\boxed{k^2 = k_\rho^2 \left\|\nabla\rho\right\|^2 - 2k_\rho \left\|\nabla\rho\right\| \frac{m\sin\alpha}{r} + \frac{m^2}{r^2} + \frac{n^2}{R^2}} \tag{48}$$

From k^2 and $k_{\parallel}$ the perpendicular wave vector is derived

$$k_\perp^2 = k^2 - k_{\parallel}^2 \tag{49}$$

Rearranging terms yields

$$k_\perp^2 = \left(k_\rho \left\|\nabla\rho\right\| - \sin\alpha \frac{m}{r}\right)^2 + \left(\sigma_B \cos\alpha T \frac{m}{r} - \sigma_I P \frac{n}{R}\right)^2 \tag{50}$$

4.5 Derivatives

Since the coordinate system is defined we can derive the expressions for the derivatives in (34)

$$\frac{\partial N_{\parallel}}{\partial \mathbf{Y}}; \frac{\partial N_\perp}{\partial \mathbf{Y}}; \frac{\partial \beta_{Ts}}{\partial \mathbf{Y}}; \frac{\partial \overline{\omega}_{ps}}{\partial \mathbf{Y}}; \frac{\partial \overline{\omega}_{cs}}{\partial \mathbf{Y}}$$

where $\mathbf{Y} = (\rho, \theta, \phi, k_\rho, m, n, t, \omega)$. The derivatives of the index of refraction are computed using (46) and (48) using $\mathbf{N} = \mathbf{k}c/\omega$ and

$$\frac{\partial N_\perp}{\partial \mathbf{Y}} = \frac{1}{2N_\perp}\left(\frac{\partial N^2}{\partial \mathbf{Y}} - 2N_{\parallel}\frac{\partial N_{\parallel}}{\partial \mathbf{Y}}\right) \tag{51}$$

. The equilibrium properties are by definition function of $(\mathbf{X}, t)$ only such that

$$\frac{\partial \beta_{Ts}}{\partial \mathbf{k}} = \frac{\partial \overline{\omega}_{ps}}{\partial \mathbf{k}} = \frac{\partial \overline{\omega}_{cs}}{\partial \mathbf{k}} = 0 \tag{52}$$

and since β_{Ts} is independent of ω

$$\frac{\partial \beta_{Ts}}{\partial \omega} = 0 \tag{53}$$

Since we consider a constant axisymmetric equilibrium

$$\frac{\partial \beta_{Ts}}{\partial t} = \frac{\partial \overline{\omega}_{ps}}{\partial t} = \frac{\partial \overline{\omega}_{cs}}{\partial t} = 0 \tag{54}$$

$$\frac{\partial \beta_{Ts}}{\partial \phi} = \frac{\partial \overline{\omega}_{ps}}{\partial \phi} = \frac{\partial \overline{\omega}_{cs}}{\partial \phi} = 0 \tag{55}$$

The the temperature and density are flux coordinates such that

$$\frac{\partial \beta_{Ts}}{\partial \theta} = \frac{\partial \overline{\omega}_{ps}}{\partial \theta} = 0 \tag{56}$$

and we are left with calculating numerically

$$\frac{\partial \beta_{Ts}}{\partial \rho}; \frac{\partial \overline{\omega}_{ps}}{\partial \rho}; \frac{\partial \overline{\omega}_{cs}}{\partial \rho}; \frac{\partial \overline{\omega}_{cs}}{\partial \theta}; \frac{\partial \overline{\omega}_{ps}}{\partial \omega}; \frac{\partial \overline{\omega}_{cs}}{\partial \omega} \tag{57}$$

Explicit expressions for these derivatives are found in Appendix 1.2.

4.6 Specular reflection at the plasma edge

Sometimes a wave is to be reflected within the scrape-off layer, which is outside the domain of application of the code. In this case, a specular reflection is enforced just before the last closed flux-surface at the location $(\rho_1, \theta_1, \phi_1)$ where the incident wave vector is $(k_{\rho 1}, m_1, n_1)$. The condition for the specular reflection is

$$\begin{array}{l} \mathbf{k}_2 \cdot \widehat{\rho} = -\mathbf{k}_1 \cdot \widehat{\rho} \\ \mathbf{k}_2 \cdot \widehat{\mathbf{s}} = \mathbf{k}_1 \cdot \widehat{\mathbf{s}} \\ \mathbf{k}_2 \cdot \widehat{\phi} = \mathbf{k}_1 \cdot \widehat{\phi} \end{array} \tag{58}$$

with the contravariant basis $\mathbf{e}^j = \left(\|\nabla\rho\| \, \widehat{\rho}, \frac{\widehat{\theta}}{r}, \frac{\widehat{\phi}}{R} \right)$ such that

$$\mathbf{k} = k_\rho \|\nabla\rho\| \, \widehat{\rho} + \frac{m}{r}\widehat{\theta} + \frac{n}{R}\widehat{\phi} \tag{59}$$

and (58) becomes

$$\begin{array}{l} k_{2\rho} \|\nabla\rho\| - \dfrac{m_2}{r} \sin\alpha = -k_{1\rho} \|\nabla\rho\| + \dfrac{m_1}{r} \sin\alpha \\ \dfrac{m_2}{r} \cos\alpha = \dfrac{m_1}{r} \cos\alpha \\ \dfrac{n_2}{R} = \dfrac{n_1}{R} \end{array} \tag{60}$$

such that m and n are conserved through the reflection and

$$k_{2\rho} \|\nabla\rho\| = 2\frac{m}{r} \sin\alpha - k_{1\rho} \|\nabla\rho\| \tag{61}$$

We should verify that the dispersion relation is satisfied for the outgoing wave. We have (46), (50)

$$\begin{array}{l} k_\parallel = \sigma_I P \cos\alpha \dfrac{m}{r} + \sigma_B T \dfrac{n}{R} \\ k_\perp = \sqrt{\left(k_\rho \|\nabla\rho\| - \sin\alpha \dfrac{m}{r} \right)^2 + \left(\sigma_B T \cos\alpha \dfrac{m}{r} - \sigma_I P \dfrac{n}{R} \right)^2} \end{array} \tag{62}$$

such that

$$\begin{array}{l} k_{\parallel 2} = k_{\parallel 1} \\ k_{\perp 2} = \sqrt{\left(\dfrac{m}{r} \sin\alpha - k_{1\rho} \|\nabla\rho\| \right)^2 + \left(\sigma_B T \cos\alpha \dfrac{m}{r} - \sigma_I P \dfrac{n}{R} \right)^2} = k_{\perp 1} \end{array} \tag{63}$$

and the dispersion relation is satisfied.

4.7 Inward propagating ray

The equation (128) for k_ρ has two solutions corresponding to inward and outward propagating waves. The solution is chosen such that the ray initially propagates inward, meaning

$$\frac{d\rho}{dt} < 0 \tag{64}$$

We have

$$\frac{d\rho}{dt} = \frac{\partial \mathcal{D}}{\partial k_\rho} \Big/ \frac{\partial \mathcal{D}}{\partial \omega} \tag{65}$$

where

$$\frac{\partial \mathcal{D}}{\partial k_\rho} = \frac{\partial N_\perp}{\partial k_\rho} \frac{\partial \mathcal{D}}{\partial N_\perp} \tag{66}$$

since $N_\parallel$ is independent of k_ρ. For positive energy waves with $\partial \mathcal{D}/\partial \omega > 0$ the condition (64) thus becomes,

$$\frac{\partial N_\perp}{\partial k_\rho} \frac{\partial \mathcal{D}}{\partial N_\perp} < 0 \tag{67}$$

We have (50)

$$\frac{\partial N_\perp}{\partial k_\rho} = \frac{c \left\| \nabla \rho \right\|}{\omega k_\perp} \left(k_\rho \left\| \nabla \rho \right\| - \sin\alpha \frac{m}{r} \right) \tag{68}$$

In general $|k_\rho| \left\| \nabla \rho \right\| > \dfrac{|m \sin\alpha|}{r}$ such that (67) reduces to

$$k_\rho \frac{\partial \mathcal{D}}{\partial N_\perp} < 0 \tag{69}$$

or equivalently

$$\boxed{k_\rho S_\perp < 0} \tag{70}$$

where $S_\perp$ is the energy flow density in the perpendicular direction.

5 Numerical algorithms

5.1 Magnetic equilibrium interpolation

Since magnetic equilibrium codes give field components on a discrete two dimensional grid mesh (ψ, θ), it is necessary to perform a numerical interpolation at the ray location. This procedure must be fast and very accurate an including first and second derivatives upon which the ray-tracing is very sensitive. Indeed, coarse interpolation may lead to large cumulative errors along the ray path and, ultimately, a wrong trajectory.

Among several methods[2], the combination of Fourier expansion and spline interpolation is chosen, taking into account of the periodic nature of the poloidal angle θ. Any

[2]Note that this method is universal, and may be used from any numerical data provided from a Grad Shafranov equation solver. However, for some codes that use finite elements techniques, it may be useful to use those directly instead of performing an additional interpolation procedure based on a spline-Fourier expansion. Indeed, finite elements contain all data needed for calculating magnetic field values at any radial and poloidal position including and first and second derivatives with an excellent accuracy. The choice to use the spline-Fourier expansion is here justified by the need to have a ray-tracing solver as general as possible.

function $g(\psi,\theta)$ is expressed as a Fourier sum

$$g(\psi,\theta) = a_0(\psi) + \sum_{n=1}^{n=N} a_n^c(\psi)\cos(n\theta) + a_n^s(\psi)\sin(n\theta) \tag{71}$$

where $N \leq N_\theta/2$ according to the Shannon theorem where N_θ is the number of discrete poloidal values. The Fourier $a_n^{(c,s)}(\psi_i)$ coefficients are determined on each discrete magnetic flux surface ψ_i in order to satisfy

$$g(\psi_i,\theta_j) = a_{0,i} + \sum_{n=1}^{n=N} a_{n,i}^c\cos(n\theta_j) + a_{n,i}^s\sin(n\theta_j) \tag{72}$$

then the coefficients $a_n^{(c,s)}(\psi)$ at any radial position $\psi_i < \psi < \psi_{i+1}$ are obtained using a usual cubic spline interpolation

$$a_n^{(c,s)}(\psi) = \alpha_{n,i}^{(c,s)}\psi^3 + \beta_{n,i}^{(c,s)}\psi^2 + \gamma_{n,i}^{(c,s)}\psi + \delta_{n,i}^{(c,s)} \tag{73}$$

the 3$^{\text{rd}}$ order polynomial coefficients being calculated so that at all nodes ψ_i, $a_n^{(c,s)}(\psi)$ is continuous, as well as its first and second derivatives.

Then the derivatives at any (ψ,θ) position are obtained from the relations

$$\begin{aligned}
\frac{\partial g(\psi,\theta)}{\partial\theta} &= \sum_{n=1}^{n=N} n\left[-a_n^c(\psi)\sin(n\theta) + a_n^s(\psi)\cos(n\theta)\right] \\
\frac{\partial^2 g(\psi,\theta)}{\partial\theta^2} &= \sum_{n=1}^{n=N} -n^2\left[a_n^c(\psi)\cos(n\theta) + a_n^s(\psi)\sin(n\theta)\right] \\
\frac{\partial g(\psi,\theta)}{\partial\psi} &= \frac{da_0^c(\psi)}{d\psi} + \sum_{n=1}^{n=N}\frac{da_n^c(\psi)}{d\psi}\cos(n\theta) + \frac{da_n^s(\psi)}{d\psi}\sin(n\theta) \\
\frac{\partial^2 g(\psi,\theta)}{\partial\psi^2} &= \frac{d^2a_0^c(\psi)}{d\psi^2} + \sum_{n=1}^{n=N}\frac{d^2a_n^c(\psi)}{d\psi^2}\cos(n\theta) + \frac{d^2a_n^s(\psi)}{d\psi^2}\sin(n\theta) \\
\frac{\partial^2 g(\psi,\theta)}{\partial\psi\partial\theta} &= \frac{da_0^c(\psi)}{d\psi} + \sum_{n=1}^{n=N} n\left[-\frac{da_n^c(\psi)}{d\psi}\sin(n\theta) + \frac{da_n^s(\psi)}{d\psi}\cos(n\theta)\right]
\end{aligned} \tag{74}$$

where

$$\begin{aligned}
\frac{da_n^{(c,s)}(\psi)}{d\psi} &= 3\alpha_{n,i}^{(c,s)}\psi^2 + 2\beta_{n,i}^{(c,s)}\psi + \gamma_{n,i}^{(c,s)} \\
\frac{d^2a_n^{(c,s)}(\psi)}{d\psi^2} &= 6\alpha_{n,i}^{(c,s)}\psi + 2\beta_{n,i}^{(c,s)}
\end{aligned} \tag{75}$$

Note that for density and temperature profiles only a cubic spline interpolation is performed, since these parameters are function of ψ only. With typically 65 poloidal angle values and 101 radial discrete positions, the relative accuracy of the magnetic equilibrium is of the order of 10^{-4} approximately. Larger numerical errors may occur near a X-point,

where the local curvature radius of all magnetic flux surfaces becomes very small. In that case and if a more detailed interpolated magnetic reconstruction is required, more poloidal points must be used in this region of the plasma, keeping the same total number of poloidal values on a non-uniform grid. When some smoothing is needed, it is always possible to use less coefficients in the Fourier expansion series.

5.2 Runge-Kutta differential equation solver

Relations (39-40) form a system of first order coupled differential equations. Knowing the initial wave characteristics $(k_{\psi 0}, m_0, n_0)$ at the position $(\psi_0, \theta_0, \phi_0)$, the problem is to evaluate (k_ψ, m, n) and (ψ, θ, ϕ) at all values of the time parameter t.

There are several algorithms for solving this initial value problem, minimizing propagation of the numerical error. One of the most popular is the Runge-Kutta algorithm which belongs to the Euler-Cauchy algorithm family[3]. The procedure consists in solving the differential equations of the type $y'(x) = f(x, y(x))$ by an iterative method, with the recurrence rule

$$y_{n+1} = y_n + h\varphi(x_n, y_n, h) \tag{76}$$

and the initial condition $y_0 = y(x_0)$.

A solution of the following form is seeked

$$\varphi(x, y, h) = \alpha_1 f(x, y(x)) + \alpha_2 f(x + \alpha h, y + \beta h f(x, y)) \tag{77}$$

so that no numerical derivatives need to be calculated. From a Taylor series expansion of $y(x)$ up to the second order, one obtains

$$\frac{y(x+h) - y(x)}{h} = y'(x) + \frac{h}{2} y''(x) + O\left(h^2\right) \tag{78}$$

$$= f(x, y) + \frac{h}{2} f^{(1)}(x, y) + O\left(h^2\right) \tag{79}$$

where

$$f^{(1)}(x, y) = \frac{\partial f}{\partial x} + f\frac{\partial f}{\partial y} \tag{80}$$

A similar expansion gives

$$f(x + \alpha h, y + \beta h f(x, y)) = f + \alpha h \frac{\partial f}{\partial x} + \beta h f \frac{\partial f}{\partial y} + O\left(h^2\right) \tag{81}$$

Thus, up to the 2nd order, φ becomes

$$\varphi(x, y, h) = (\alpha_1 + \alpha_2) f(x, y) + h\left[\alpha\alpha_2 \frac{\partial f}{\partial x} + \beta\alpha_2 f \frac{\partial f}{\partial y}\right] + O\left(h^2\right) \tag{82}$$

so that

$$\begin{aligned} \frac{y(x+h) - y(x)}{h} - \varphi(x, y, h) = {} & (1 - \alpha_1 - \alpha_2) \\ & + h\left(\frac{1}{2} - \alpha\alpha_2\right)\frac{\partial f}{\partial x} \\ & + h\left(\frac{1}{2} - \beta\alpha_2\right)\frac{\partial f}{\partial y} + O\left(h^2\right) \end{aligned} \tag{83}$$

[3]There exists other methods used also for ray-tracing named "predictor-corrector" which belong to the general Adams algorithm family.

In order to obtain a second order accurate calculation, the coefficients must satisfy the relations

$$\begin{array}{c} \alpha_1 + \alpha_2 = 1 \\ \alpha\alpha_2 = 1/2 \\ \beta\alpha_2 = 1/2 \end{array} \tag{84}$$

which implies

$$\begin{array}{c} \alpha = \beta = \dfrac{1}{2\alpha_2} \\ \alpha_1 = 1 - \alpha_2 \end{array} \tag{85}$$

The solution is finally

$$\varphi(x, y, h) = (1 - \alpha) f(x, y) + \alpha f\left(x + \frac{h}{2\alpha}, y + \frac{h}{2\alpha} f(x, y)\right) \tag{86}$$

where the case $\alpha = 1/2$ corresponds to the Eun's algorithm, while $\alpha = 1$ is corresponding to the modified Euler's algorithm.

A second order Runge-Kutta algorithm then corresponds to the following procedure,

$$\begin{array}{c} y_{n+1} = y_n + h\varphi(x_n, y_n, h) \\ \varphi(x_n, y_n, h) = (1 - \alpha) k_1 + \alpha k_2 \\ k_1 = f(x, y) \\ k_2 = f\left(x + \dfrac{h}{2\alpha}, y + \dfrac{h}{2\alpha} k_1\right) \end{array} \tag{87}$$

The parameter α is chosen depending upon the studied problem, and parameter h, which must be small, may be adjusted at each iteration step, as function of the local curvature of the ray path. This is the adaptative Runge-Kutta method, widely used for solving this type of problem.

This procedure, which has been highlighted for order 2, may be expanded in a similar manner to higher orders. Detailed calculations can be found in the literature [11].

In the ray-tracing code, a sixth order adaptative Runge-Kutta integration method is used. The numerical accuracy obtained with this method is very satisfactory, and the condition $|\mathcal{D}| \leq 10^{-10}$ is usually obtained along the ray path, despite a sudden increase in $|\mathcal{D}|$ sometimes observed near the cold/fast wave mode conversion.

6 Conclusion

The code *C3PO* has been designed for fast and accurate calculations of the ray trajectories in inhomogeneous and anisotropic plasmas with arbitrary axisymmetric magnetic equilibrium and nested flux surfaces. It is part of the *C3PO/LUKE/R5-X2* codes package designed for calculating RF current drive in tokamaks or reverse field pinches. A modular structure makes the code evolutive. In particular, additional dielectric response models can be implemented.

Among possible future improvements, *C3PO* could be developed into a beam tracing code to include diffraction effects and calculate the beam size. It could also be extended to account for toroidal equilibrium inhomogeneities such as the magnetic ripple [3, 4].

A Explicit expressions

A.1 Dispersion relation

In a cartesian system (x, y, z) defined such that the background magnetic field is

$$\mathbf{B}_0 = B_0 \hat{\mathbf{z}} \tag{88}$$

and the wave index of refraction is

$$\mathbf{N} = N_\parallel \hat{\mathbf{z}} + N_\perp \hat{\mathbf{x}} \tag{89}$$

the permittivity tensor can be expressed explicitly as

$$\mathbb{K} = \begin{pmatrix} K_{xx} & K_{xy} & K_{xz} \\ -K_{xy} & K_{yy} & K_{yz} \\ K_{xz} & -K_{yz} & K_{zz} \end{pmatrix} \tag{90}$$

such that the dispersion tensor is

$$\mathbb{D} = \begin{pmatrix} K_{xx} - N_\parallel^2 & K_{xy} & K_{xz} + N_\perp N_\parallel \\ -K_{xy} & K_{yy} - N^2 & K_{yz} \\ K_{xz} + N_\perp N_\parallel & -K_{yz} & K_{zz} - N_\perp^2 \end{pmatrix} \tag{91}$$

and the dispersion relation becomes

$$\begin{aligned} \mathcal{D}(\mathbf{k}, \omega) = & \left(K_{xx} - N_\parallel^2\right)\left(K_{yy} - N^2\right)\left(K_{zz} - N_\perp^2\right) \\ & + 2K_{xy}K_{yz}\left(K_{xz} + N_\perp N_\parallel\right) \\ & - \left(K_{yy} - N^2\right)\left(K_{xz} + N_\perp N_\parallel\right)^2 \\ & + K_{yz}^2\left(K_{xx} - N_\parallel^2\right) + K_{xy}^2\left(K_{zz} - N_\perp^2\right) \end{aligned} \tag{92}$$

$\mathcal{D}(\mathbf{k}, \omega)$ is rearranged in powers of $N_\perp$ as

$$\mathcal{D}(\mathbf{k}, \omega) = P_4 N_\perp^4 + P_3 N_\perp^3 + P_2 N_\perp^2 + P_1 N_\perp + P_0 \tag{93}$$

with

$$\begin{aligned} P_4 &= K_{xx} \\ P_3 &= 2K_{xz}N_\parallel \\ P_2 &= \left(K_{xx} + K_{zz}\right)N_\parallel^2 - \left(K_{yy} + K_{zz}\right)K_{xx} + K_{xz}^2 - K_{xy}^2 \\ P_1 &= 2N_\parallel\left(K_{xz}N_\parallel^2 + K_{xy}K_{yz} - K_{yy}K_{xz}\right) \\ P_0 &= N_\parallel^4 K_{zz} + \left(K_{xz}^2 - K_{yz}^2 - \left[K_{xx} + K_{yy}\right]K_{zz}\right)N_\parallel^2 + K_{yy}K_{xx}K_{zz} \\ &\quad + 2K_{xy}K_{yz}K_{xz} + K_{yz}^2 K_{xx} - K_{yy}K_{xz}^2 + K_{xy}^2 K_{zz} \end{aligned} \tag{94}$$

The dispersion relation (93) can be further expanded as

$$\begin{aligned}
\mathcal{D} = & \left(1 + X_{xx}\right) N_\perp^4 \\
& + \left(2 N_\parallel X_{xz}\right) N_\perp^3 \\
& + \left(N_\parallel^2 \left(X_{xx} + X_{zz} + 2\right) - 2X_{xx} - X_{yy} - X_{zz}\right. \\
& \left. - X_{xx}X_{zz} + X_{xz}^2 - X_{xx}X_{yy} - X_{xy}^2 - 2\right) N_\perp^2 \\
& + 2N_\parallel \left(-X_{yy}X_{xz} + X_{xy}X_{yz} - X_{xz} + N_\parallel^2 X_{xz}\right) N_\perp \\
& + 1 + N_\parallel^4 \left(X_{zz} + 1\right) \\
& + N_\parallel^2 \left(X_{xz}^2 - X_{yy}X_{zz} - X_{xx}X_{zz} - 2X_{zz} - X_{yy} - X_{yz}^2 - X_{xx} - 2\right) \\
& + X_{yy}X_{zz} + X_{xx}X_{zz} + X_{xx}X_{yy} \\
& + X_{xx}X_{yz}^2 + X_{yz}^2 + X_{xx} + X_{xy}^2 + X_{xy}^2 X_{zz} - X_{xz}^2 \\
& - X_{yy}X_{xz}^2 + X_{yy} + X_{zz} \\
& + X_{xx}X_{yy}X_{zz} + 2X_{xy}X_{yz}X_{xz}
\end{aligned} \tag{95}$$

In preparation for calculating the derivatives, it is useful to split the dispersion relation in a sum of products

$$\mathcal{D} = \sum_{k=1}^{k=43} \mathcal{D}^{(k)} \tag{96}$$

where

$$\begin{aligned}
\mathcal{D}^{(1)} &= N_\perp^4 \\
\mathcal{D}^{(2)} &= X_{xx} N_\perp^4 \\
\mathcal{D}^{(3)} &= 2N_\parallel X_{xz} N_\perp^3 \\
\mathcal{D}^{(4)} &= N_\parallel^2 X_{xx} N_\perp^2 \\
\mathcal{D}^{(5)} &= N_\parallel^2 X_{zz} N_\perp^2 \\
\mathcal{D}^{(6)} &= 2N_\parallel^2 N_\perp^2 \\
\mathcal{D}^{(7)} &= -2X_{xx} N_\perp^2 \\
\mathcal{D}^{(8)} &= -X_{yy} N_\perp^2 \\
\mathcal{D}^{(9)} &= -X_{zz} N_\perp^2 \\
\mathcal{D}^{(10)} &= -X_{xx}X_{zz} N_\perp^2
\end{aligned} \tag{97}$$

$$\begin{aligned}
\mathcal{D}^{(11)} &= X_{xz}^2 N_\perp^2 \\
\mathcal{D}^{(12)} &= -X_{xx}X_{yy} N_\perp^2 \\
\mathcal{D}^{(13)} &= -X_{xy}^2 N_\perp^2 \\
\mathcal{D}^{(14)} &= -2N_\perp^2 \\
\mathcal{D}^{(15)} &= -2N_\parallel X_{yy}X_{xz} N_\perp \\
\mathcal{D}^{(16)} &= 2N_\parallel X_{xy}X_{yz} N_\perp \\
\mathcal{D}^{(17)} &= -2N_\parallel X_{xz} N_\perp \\
\mathcal{D}^{(18)} &= 2N_\parallel^3 X_{xz} N_\perp \\
\mathcal{D}^{(19)} &= 1 \\
\mathcal{D}^{(20)} &= N_\parallel^4 X_{zz}
\end{aligned} \tag{98}$$

$$
\begin{aligned}
\mathcal{D}^{(21)} &= N_{\parallel}^{4} \\
\mathcal{D}^{(22)} &= N_{\parallel}^{2} X_{xz}^{2} \\
\mathcal{D}^{(23)} &= -N_{\parallel}^{2} X_{yy} X_{zz} \\
\mathcal{D}^{(24)} &= -N_{\parallel}^{2} X_{xx} X_{zz} \\
\mathcal{D}^{(25)} &= -2N_{\parallel}^{2} X_{zz} \\
\mathcal{D}^{(26)} &= -N_{\parallel}^{2} X_{yy} \\
\mathcal{D}^{(27)} &= -N_{\parallel}^{2} X_{yz}^{2} \\
\mathcal{D}^{(28)} &= -N_{\parallel}^{2} X_{xx} \\
\mathcal{D}^{(29)} &= -2N_{\parallel}^{2} \\
\mathcal{D}^{(30)} &= X_{yy} X_{zz}
\end{aligned}
\tag{99}
$$

$$
\begin{aligned}
\mathcal{D}^{(31)} &= X_{xx} X_{zz} \\
\mathcal{D}^{(32)} &= X_{xx} X_{yy} \\
\mathcal{D}^{(33)} &= X_{xx} X_{yz}^{2} \\
\mathcal{D}^{(34)} &= X_{yz}^{2} \\
\mathcal{D}^{(35)} &= X_{xx} \\
\mathcal{D}^{(36)} &= X_{xy}^{2} \\
\mathcal{D}^{(37)} &= X_{xy}^{2} X_{zz} \\
\mathcal{D}^{(38)} &= -X_{xz}^{2} \\
\mathcal{D}^{(39)} &= -X_{yy} X_{xz}^{2} \\
\mathcal{D}^{(40)} &= X_{yy}
\end{aligned}
\tag{100}
$$

$$
\begin{aligned}
\mathcal{D}^{(41)} &= X_{zz} \\
\mathcal{D}^{(42)} &= X_{xx} X_{yy} X_{zz} \\
\mathcal{D}^{(43)} &= 2X_{xy} X_{yz} X_{xz}
\end{aligned}
\tag{101}
$$

A.2 Derivatives of the equilibrium

Explicitly expression for derivatives of the equilibrium are

$$
\frac{\partial \beta_{Ts}}{\partial \rho} = \frac{\partial}{\partial \rho}\left(\sqrt{\frac{\kappa T_s}{m_s c^2}}\right) = \frac{\beta_{Ts}}{2T_s}\frac{\partial T_s}{\partial \rho} \tag{102}
$$

$$
\frac{\partial \overline{\omega}_{ps}}{\partial \rho} = \frac{\partial}{\partial \rho}\left(\frac{1}{\omega}\sqrt{\frac{q_s^2 n_s}{\varepsilon_0 m_s}}\right) = \frac{\overline{\omega}_{ps}}{2n_s}\frac{\partial n_s}{\partial \rho} \tag{103}
$$

$$
\frac{\partial \overline{\omega}_{cs}}{\partial \rho} = \frac{\partial}{\partial \rho}\left(\frac{q_s B_0}{m_s \omega}\right) = \frac{\overline{\omega}_{cs}}{B_0}\frac{\partial B_0}{\partial \rho} \tag{104}
$$

$$
\frac{\partial \overline{\omega}_{cs}}{\partial \theta} = \frac{\partial}{\partial \theta}\left(\frac{q_s B_0}{m_s \omega}\right) = \frac{\overline{\omega}_{cs}}{B_0}\frac{\partial B_0}{\partial \theta} \tag{105}
$$

$$
\frac{\partial \overline{\omega}_{ps}}{\partial \omega} = \frac{\partial}{\partial \omega}\left(\frac{1}{\omega}\sqrt{\frac{q_s^2 n_s}{\varepsilon_0 m_s}}\right) = -\frac{\overline{\omega}_{ps}}{\omega} \tag{106}
$$

$$
\frac{\partial \overline{\omega}_{cs}}{\partial \omega} = \frac{\partial}{\partial \omega}\left(\frac{q_s B_0}{m_s \omega}\right) = -\frac{\overline{\omega}_{cs}}{\omega} \tag{107}
$$

B Various properties of the coordinates system

B.1 Alternative calculation of the parallel index of refraction

The following expression is considered

$$k_{\parallel} = \frac{1}{B}\mathbf{k}\cdot\mathbf{B} \tag{108}$$

$$= \frac{1}{B}g^{ij}k_i B_j \tag{109}$$

with the metric coefficients

$$g^{ij} = \mathbf{e}^i\cdot\mathbf{e}^j = \begin{pmatrix} \|\nabla\rho\|^2 & -\frac{\|\nabla\rho\|\sin\alpha}{r} & 0 \\ -\frac{\|\nabla\rho\|\sin\alpha}{r} & \frac{1}{r^2} & 0 \\ 0 & 0 & \frac{1}{R^2} \end{pmatrix} \tag{110}$$

The magnetic field in the covariant basis

$$\mathbf{e}_i = \left(\frac{\widehat{\mathbf{r}}}{\|\nabla\rho\|\cos\alpha}, \frac{r\widehat{\mathbf{s}}}{\cos\alpha}, R\widehat{\phi}\right) \tag{111}$$

has the following coordinates

$$B_j = \left(\sigma_I\frac{\sin\alpha B_P}{\|\nabla\rho\|\cos\alpha}, \sigma_I\frac{rB_P}{\cos\alpha}, \sigma_B RB_T\right) \tag{112}$$

such that

$$k_{\parallel} = \frac{1}{B}\left(k_\psi, m, n\right)\begin{pmatrix} \|\nabla\rho\|^2 & -\frac{\|\nabla\rho\|\sin\alpha}{r} & 0 \\ -\frac{\|\nabla\rho\|\sin\alpha}{r} & \frac{1}{r^2} & 0 \\ 0 & 0 & \frac{1}{R^2} \end{pmatrix}\begin{pmatrix} \sigma_I\frac{\sin\alpha B_P}{\|\nabla\rho\|\cos\alpha} \\ \frac{rB_P}{\cos\alpha} \\ \sigma_B RB_T \end{pmatrix} \tag{113}$$

which gives

$$k_{\parallel} = \frac{1}{B}\left[\left(k_\rho\|\nabla\rho\|^2 - \frac{m\|\nabla\rho\|\sin\alpha}{r}\right)\sigma_I\frac{\sin\alpha B_P}{\|\nabla\rho\|\cos\alpha} + \left(-\frac{\|\nabla\rho\|\sin\alpha}{r}k_\rho + \frac{m}{r^2}\right)\sigma_I\frac{rB_P}{\cos\alpha} + \frac{n\sigma_B}{R^2}RB_T\right] \tag{114}$$

and simplifies to

$$k_{\parallel} = \left[\sigma_I\cos\alpha P\frac{m}{r} + \sigma_B T\frac{n}{R}\right] \tag{115}$$

B.2 Calculation of k_ρ, m and/or n as a function of $k_{\parallel}$ and $k_\perp$

Generally, the initial conditions determine m and $k_{\parallel}$. Then $k_\perp$ is calculated from the dispersion relation. We need to express k_ρ and n as a function of m, $k_{\parallel}$ and $k_\perp$. We have

$$k_\perp^2 = k_\rho^2\|\nabla\rho\|^2 - 2k_\rho\|\nabla\rho\|\frac{m\sin\alpha}{r} + \frac{m^2}{r^2} + \frac{n^2}{R^2} - k_{\parallel}^2 \tag{116}$$

and

$$k_{\parallel} = \sigma_I P \cos\alpha \frac{m}{r} + \sigma_B T \frac{n}{R} \tag{117}$$

We get an expression for n

$$n = \sigma_B \frac{R}{T}\left(k_{\parallel} - \sigma_I P \cos\alpha \frac{m}{r}\right) \tag{118}$$

which is inserted back in (116) to get

$$k_{\perp}^2 = k_{\rho}^2 \left\|\nabla\rho\right\|^2 - 2\sin\alpha \frac{m}{r} k_{\rho} \left\|\nabla\rho\right\| + \frac{m^2}{r^2} + \frac{1}{T^2}\left(k_{\parallel} - \sigma_I P \cos\alpha \frac{m}{r}\right)^2 - k_{\parallel}^2 \tag{119}$$

and k_{ρ} is solution of the equation

$$k_{\rho}^2 \left\|\nabla\rho\right\|^2 - 2\sin\alpha \frac{m}{r} k_{\rho} \left\|\nabla\rho\right\| + \left(1 + \frac{P^2}{T^2}\cos^2\alpha\right)\frac{m^2}{r^2} + \frac{P^2}{T^2}k_{\parallel}^2 - 2\sigma_I \frac{P}{T^2}\cos\alpha \frac{m}{r} k_{\parallel} - k_{\perp}^2 = 0 \tag{120}$$

Defining

$$X = k_{\rho}\left\|\nabla\rho\right\| \tag{121}$$

and

$$B = \sin\alpha \frac{m}{r} \tag{122}$$

$$C = \left(1 + \frac{P^2}{T^2}\cos^2\alpha\right)\frac{m^2}{r^2} + \frac{P^2}{T^2}k_{\parallel}^2 - 2\sigma_I \frac{P}{T^2}\frac{m}{r}k_{\parallel}\cos\alpha - k_{\perp}^2 \tag{123}$$

we have

$$X^2 - 2BX + C = 0 \tag{124}$$

such that

$$X = B \pm \sqrt{B^2 - C} \tag{125}$$

which gives

$$k_{\rho} = \frac{1}{\left\|\nabla\rho\right\|}\left[\sin\alpha\frac{m}{r} \pm \sqrt{k_{\perp}^2 - \frac{1}{T^2}\left(\cos\alpha\frac{m}{r} - \sigma_I P k_{\parallel}\right)^2}\right] \tag{126}$$

To sum up

$$\boxed{\begin{array}{l} n = \sigma_B \dfrac{R}{T}\left(k_{\parallel} - \sigma_I P \cos\alpha \dfrac{m}{r}\right) \\ m = \sigma_I \dfrac{1}{P\cos\alpha}\left(k_{\parallel} - \sigma_B T \dfrac{n}{R}\right) \\ k_{\rho} = \dfrac{1}{\left\|\nabla\rho\right\|}\left[\sin\alpha\dfrac{m}{r} + \sigma_{\rho}\sqrt{k_{\perp}^2 - \dfrac{1}{T^2}\left(\cos\alpha\dfrac{m}{r} - \sigma_I P k_{\parallel}\right)^2}\right] \end{array}} \tag{127}$$

where $\sigma_{\rho} = \pm 1$. We can also express k_{ρ} as

$$\boxed{k_{\rho} = \frac{1}{\left\|\nabla\rho\right\|}\left[\sin\alpha\frac{m}{r} + \sigma_{\rho}\sqrt{k^2 - \cos^2\alpha\frac{m^2}{r^2} - \frac{n^2}{R^2}}\right]} \tag{128}$$

The correct solution for k_{ρ} can be determined from (70).

B.3 Calculation of k_ρ, m and n as a function of k_R, k_Z and k_ϕ

The vector $\mathbf{k}$ is projected onto the covariant basis

$$\mathbf{e}_i = \left(\frac{\hat{\mathbf{r}}}{\|\nabla\rho\| \cos\alpha}, \frac{r\hat{\mathbf{s}}}{\cos\alpha}, R\hat{\phi} \right) \tag{129}$$

such that

$$\begin{array}{l} k_\rho = \dfrac{\hat{\mathbf{r}} \cdot \mathbf{k}}{\|\nabla\rho\| \cos\alpha} \\ m = \dfrac{r\hat{\mathbf{s}} \cdot \mathbf{k}}{\cos\alpha} \\ n = R\hat{\phi} \cdot \mathbf{k} \end{array} \tag{130}$$

If $\mathbf{k}$ is expressed in coordinates (R, Z, ϕ) as $\mathbf{k} = k_R\hat{\mathbf{R}} + k_Z\hat{\mathbf{Z}} + k_\phi\hat{\phi}$ or in coordinates (r, θ, ϕ) as $\mathbf{k} = k_r\hat{\mathbf{r}} + k_\theta\hat{\theta} + k_\phi\hat{\phi}$ we get

$$\begin{array}{l} k_\rho = \dfrac{k_r}{\|\nabla\rho\| \cos\alpha} \\ m = r\left(k_\theta + k_r \tan\alpha\right) \\ n = Rk_\phi \end{array} \tag{131}$$

where

$$\begin{array}{l} k_r = k_R \cos\theta + k_Z \sin\theta \\ k_\theta = -k_R \sin\theta + k_Z \cos\theta \end{array} \tag{132}$$

Note that we retrieve

$$\begin{array}{l} k_\parallel = \sigma_I P \left(\hat{\mathbf{s}} \cdot \mathbf{k}\right) + \sigma_B T \left(\hat{\phi} \cdot \mathbf{k}\right) = \dfrac{\mathbf{B} \cdot \mathbf{k}}{\|\mathbf{B}\|} \\ k_\perp = \sqrt{\left[\left(\hat{\rho} \cdot \mathbf{k}\right)^2 + \left(\hat{\mathbf{s}} \cdot \mathbf{k}\right)^2 + \left(\hat{\phi} \cdot \mathbf{k}\right)^2 - k_\parallel^2 \right]} = \sqrt{k^2 - k_\parallel^2} \end{array} \tag{133}$$

since

$$\begin{array}{l} \hat{\mathbf{s}} \cdot \mathbf{k} = \sin\alpha k_r + \cos\alpha k_\theta \\ \hat{\rho} \cdot \mathbf{k} = \cos\alpha k_r - \sin\alpha k_\theta \end{array} \tag{134}$$

B.4 Wave scattering by fluctuations

Low frequency fluctuations of the electron density or the magnetic field can strongly affect the propagation of rf waves in a magnetized plasma. This effect has been extensively investigated for the Lower Hybrid wave by solving a wave kinetic equation in the weak turbulence approximation. [14, 15]. In this approach, the flow of rf energy is described by a usual ray-tracing between random scattering events where the initial wave vector $\mathbf{k}$ can be modified both in amplitude and direction with the constraint to remain solution of the local dispersion relation. This physical mechanism is a good candidate for explaining a possible strong upshift of the power spectrum as the Lower Hybrid wave propagates in the plasma, even if the toroidal mode coupling for bridging the spectral gap is very weak. Though primarily dedicated to the Lower Hybrid wave, the concept of wave scattering by low frequency density or magnetic field fluctuations can be easily extended to other types of rf waves provided that $\widetilde{k}_\parallel \ll k_\parallel$ and $\widetilde{\omega} \ll \omega$, where $k_\parallel = \mathbf{k} \cdot \mathbf{b}$ and $\widetilde{k}_\parallel = \widetilde{\mathbf{k}} \cdot \mathbf{b}$ are the projections of the rf and fluctuation wave vectors respectively along the direction of the local magnetic field $\mathbf{b} = \mathbf{B}/\|\mathbf{B}\|$, while ω and $\widetilde{\omega}$ are the rf and fluctuation frequencies

respectively. Consequently, the scattering process becomes a two dimensional problem in the plane perpendicular to the local magnetic field direction, a reasonable assumption regarding the large difference between the long wave length of the low frequency fluctuations and the short length of the rf waves along $\mathbf{b}$.[4]

Calculations are organized in three steps. In the first section, the components of the scattered rf wave vector are calculated, according to the curvilinear coordinate system chosen for describing the magnetic equilibrium in C3PO. The wave kinetic equation corresponding to the wave-wave interaction is then derived from first principles in the second section. Finally, in the third section, the wave kinetic equation is solved using a Monte-Carlo method and the procedure for the numerical implementation in the code is explicited.

Before entering into the details of the calculations, it is possible to estimate the impact of a simple transfer from the toroidal mode number n to the poloidal one m at fixed $k_{\|0}$ on the ray properties, by changing the initial conditions. The benchmark case presented in Sec.E.1 is considered using $N_{\phi 0} = -1.8$. From a scan of $m \in \{-300, 300\}$ with steps $\Delta m = 50$, it is possible to show that a variation of m and n strongly affect the ray propagation, even if $k_{\|0}$ remains unchanged.

B.4.1 Calculation of the scattered wave vector

When the rf wave vector $\mathbf{k}$ is scattered by low density fluctuations, it may change both in module and direction, with the conditions

$$\mathbf{k} \cdot \mathbf{b} = \mathbf{k}' \cdot \mathbf{b} = k_{\|} \tag{135}$$

where $\mathbf{k}'$ is the scattered wave vector. Its perpendicular component $k'_{\perp} = \|\mathbf{k}'_{\perp}\|$, where $\mathbf{k}'_{\perp} = \mathbf{k}' \times \mathbf{b}$, is determined by solving the local dispersion relation (18) at fixed $k_{\|}$, and its direction results from a rotation $\mathcal{R}_{\beta}$ of an angle β around the magnetic field direction $\mathbf{b}$ so that

$$\mathbf{k}_{\perp} \cdot \mathbf{k}'_{\perp} = k_{\perp} k'_{\perp} \cos\beta \tag{136}$$

For unlike transitions, the scattered wave moves to a different branch of propagation and $k'_{\perp} \neq k_{\perp}$, otherwise $k'_{\perp} = k_{\perp}$ for like transitions. From the relations (18), (135) and (136), all the components $\left(k'_{\rho}, m', n'\right)$ of $\mathbf{k}'$ can be deduced from those of $\mathbf{k}$.[5]

The wave scattering may be therefore described as a two steps process, and the mode conversion $\mathcal{M}$ and the rotation $\mathcal{R}_{\beta}$.

B.4.2 Derivation of the wave kinetic equation

B.4.3 Solution of the wave kinetic equation

Using the Rodrigues general formula for the rotation $\mathcal{R}_{\beta}$ of a vector $\mathbf{k}$,

$$\widetilde{\mathbf{k}} = \mathcal{R}_{\beta}(\mathbf{k}) = \cos\beta \mathbf{k} + (1 - \cos\beta)(\mathbf{k} \cdot \mathbf{b})\mathbf{b} + \sin\beta(\mathbf{b} \times \mathbf{k}) \tag{137}$$

[4]The parallel wave length $\lambda_{\|}$ is related to the parallel refractive index $N_{\|}$ of the rf wave by the simple relation $\lambda_{\|} = c/fN_{\|}$,where $f = \omega/2\pi$. For the Lower Hybrid wave at $f_{LH} = 3.7GHz$ and $N_{\|LH} \simeq 2$, $\lambda_{\|LH} \simeq 2cm$. From turwhich is much less than the wave length $\widetilde{\lambda}_{\|} \simeq ***cm$ of density fluctuation along the parallel direction. For the Electron Cyclotron wave, $f_{EC} = 110GHz$ and $N_{\|EC} \simeq 0.2$, so that $\lambda_{\|EC} \simeq 2cm$ is even smaller than $\lambda_{\|LH} \simeq 2cm$ as compared to $\widetilde{\lambda}_{\|}$.

[5]In Ref. [14], the relation $\mathbf{b} \cdot (\mathbf{k}_{\perp} \times \mathbf{k}'_{\perp}) = k_{\perp} k'_{\perp} \sin\beta$ is also introduced in addition to (135) and (136). However, it is fully equivalent to (136) and does not provide any additional information.

it turns out that each components of $\widetilde{\mathbf{k}}$ is given by the relations

$$\widetilde{\mathbf{k}} \cdot \widehat{\rho} = \cos\beta \mathbf{k} \cdot \widehat{\rho} + (1 - \cos\beta)(\mathbf{k} \cdot \mathbf{b})\, \mathbf{b} \cdot \widehat{\rho} + \sin\beta\, (\mathbf{b} \times \mathbf{k}) \cdot \widehat{\rho}$$
$$\widetilde{\mathbf{k}} \cdot \widehat{\theta} = \cos\beta \mathbf{k} \cdot \widehat{\theta} + (1 - \cos\beta)(\mathbf{k} \cdot \mathbf{b})\, \mathbf{b} \cdot \widehat{\theta} + \sin\beta\, (\mathbf{b} \times \mathbf{k}) \cdot \widehat{\theta}$$
$$\widetilde{\mathbf{k}} \cdot \widehat{\phi} = \cos\beta \mathbf{k} \cdot \widehat{\phi} + (1 - \cos\beta)(\mathbf{k} \cdot \mathbf{b})\, \mathbf{b} \cdot \widehat{\phi} + \sin\beta\, (\mathbf{b} \times \mathbf{k}) \cdot \widehat{\phi}$$

Using the vectorial relations

$$(\mathbf{b} \times \mathbf{k}) \cdot \widehat{\rho} = (\widehat{\rho} \times \mathbf{b}) \cdot \mathbf{k}$$
$$(\mathbf{b} \times \mathbf{k}) \cdot \widehat{\theta} = \left(\widehat{\theta} \times \mathbf{b}\right) \cdot \mathbf{k}$$
$$(\mathbf{b} \times \mathbf{k}) \cdot \widehat{\phi} = \left(\widehat{\phi} \times \mathbf{b}\right) \cdot \mathbf{k}$$

and the expression on the magnetic field $\mathbf{b} = \sigma_B T \widehat{\phi} + \sigma_I P \hat{\mathbf{s}}$ according to the relation (36), recalling that $T = B_T/B$ and $P = B_P/B$, one obtains

$$(\mathbf{b} \times \mathbf{k}) \cdot \widehat{\rho} = \sigma_B T \left(\widehat{\rho} \times \widehat{\phi}\right) \cdot \mathbf{k} + \sigma_I P\, (\widehat{\rho} \times \hat{\mathbf{s}}) \cdot \mathbf{k}$$
$$(\mathbf{b} \times \mathbf{k}) \cdot \widehat{\theta} = \sigma_B T \left(\widehat{\theta} \times \widehat{\phi}\right) \cdot \mathbf{k} + \sigma_I P \left(\widehat{\theta} \times \hat{\mathbf{s}}\right) \cdot \mathbf{k}$$
$$(\mathbf{b} \times \mathbf{k}) \cdot \widehat{\phi} = \sigma_B T \left(\widehat{\phi} \times \widehat{\phi}\right) \cdot \mathbf{k} + \sigma_I P \left(\widehat{\phi} \times \hat{\mathbf{s}}\right) \cdot \mathbf{k}$$

which simplifies to

$$(\mathbf{b} \times \mathbf{k}) \cdot \widehat{\rho} = -\sigma_B T \hat{\mathbf{s}} \cdot \mathbf{k} + \sigma_I P \widehat{\phi} \cdot \mathbf{k}$$
$$(\mathbf{b} \times \mathbf{k}) \cdot \widehat{\theta} = \sigma_B T \widehat{\mathbf{r}} \cdot \mathbf{k} - \sigma_I P \sin\alpha \widehat{\phi} \cdot \mathbf{k}$$
$$(\mathbf{b} \times \mathbf{k}) \cdot \widehat{\phi} = -\sigma_I P \widehat{\rho} \cdot \mathbf{k}$$

since

$$\widehat{\rho} \times \widehat{\phi} = -\widehat{\mathbf{s}}$$
$$\widehat{\theta} \times \widehat{\phi} = \widehat{\mathbf{r}}$$

and

$$\widehat{\rho} \times \hat{\mathbf{s}} = \widehat{\phi}$$
$$\widehat{\theta} \times \hat{\mathbf{s}} = -\sin\alpha \widehat{\phi}$$
$$\widehat{\phi} \times \hat{\mathbf{s}} = -\widehat{\rho}$$

using the relations $\hat{\mathbf{s}} = \sin\alpha \widehat{\mathbf{r}} + \cos\alpha \widehat{\theta}$ and $\widehat{\theta} = \widehat{\phi} \times \hat{\mathbf{r}}$. Using (59),

$$\hat{\mathbf{s}} \cdot \mathbf{k} = \frac{m}{r} \cos\alpha$$
$$\widehat{\phi} \cdot \mathbf{k} = \frac{n}{R}$$
$$\widehat{\mathbf{r}} \cdot \mathbf{k} = k_\rho \left\|\nabla\rho\right\| \cos\alpha$$
$$\widehat{\rho} \cdot \mathbf{k} = k_\rho \left\|\nabla\rho\right\| - \sin\alpha \frac{m}{r}$$
$$\widehat{\theta} \cdot \mathbf{k} = -\sin\alpha k_\rho \left\|\nabla\rho\right\| + \frac{m}{r}$$

and

$$(\mathbf{b}\times\mathbf{k})\cdot\widehat{\rho}=-\sigma_B T\frac{m}{r}\cos\alpha+\sigma_I P\frac{n}{R}$$
$$(\mathbf{b}\times\mathbf{k})\cdot\widehat{\theta}=\sigma_B T k_\rho\left\|\nabla\rho\right\|\cos\alpha-\sigma_I P\sin\alpha\frac{n}{R}$$
$$(\mathbf{b}\times\mathbf{k})\cdot\widehat{\phi}=-\sigma_I P\left(k_\rho\left\|\nabla\rho\right\|-\sin\alpha\frac{m}{r}\right)$$

Finally, since

$$\mathbf{b}\cdot\widehat{\rho}=0$$
$$\mathbf{b}\cdot\widehat{\theta}=\sigma_I P\cos\alpha$$
$$\mathbf{b}\cdot\widehat{\phi}=\sigma_B T$$

one obtains

$$\widetilde{k}_\rho\left\|\nabla\rho\right\|-\sin\alpha\frac{\widetilde{m}}{r}=\cos\beta\left(k_\rho\left\|\nabla\rho\right\|-\sin\alpha\frac{m}{r}\right)+\sin\beta\left(-\sigma_B T\frac{m}{r}\cos\alpha+\sigma_I P\frac{n}{R}\right)$$
$$-\sin\alpha\widetilde{k}_\rho\left\|\nabla\rho\right\|+\frac{\widetilde{m}}{r}=\cos\beta\left(-\sin\alpha k_\rho\left\|\nabla\rho\right\|+\frac{m}{r}\right)+(1-\cos\beta)\,k_\parallel\sigma_I P\cos\alpha+\sin\beta\left(\sigma_B T k_\rho\left\|\nabla\rho\right\|\cos\alpha-\right.$$
$$\frac{\widetilde{n}}{R}=\cos\beta\frac{n}{R}+(1-\cos\beta)\,k_\parallel\sigma_B T-\sin\beta\sigma_I P\left(k_\rho\left\|\nabla\rho\right\|-\sin\alpha\frac{m}{r}\right)$$

or

$$\widetilde{k}_\rho\left\|\nabla\rho\right\|=\cos\beta k_\rho\left\|\nabla\rho\right\|+(1-\cos\beta)\,k_\parallel\sigma_I P\tan\alpha+\sin\beta\left(\frac{\sigma_B T}{\cos\alpha}\left(k_\rho\left\|\nabla\rho\right\|\sin\alpha-\frac{m}{r}\right)+\sigma_I P\frac{n}{R}\right)$$
$$\frac{\widetilde{m}}{r}=\cos\beta\frac{m}{r}+(1-\cos\beta)\,k_\parallel\frac{\sigma_I P}{\cos\alpha}+\sin\beta\frac{\sigma_B T}{\cos\alpha}\left(k_\rho\left\|\nabla\rho\right\|-\frac{m}{r}\sin\alpha\right)$$
$$\frac{\widetilde{n}}{R}=\cos\beta\frac{n}{R}+(1-\cos\beta)\,k_\parallel\sigma_B T+\sin\beta\sigma_I P\left(-k_\rho\left\|\nabla\rho\right\|+\sin\alpha\frac{m}{r}\right)\quad(138)$$

where $\mathbf{k}\cdot\mathbf{b}=k_\parallel$ and the scattered wave vector is

$$\widetilde{\mathbf{k}}=\widetilde{k}_\rho\left\|\nabla\rho\right\|\widehat{\rho}+\frac{\widetilde{m}}{r}\widehat{\theta}+\frac{\widetilde{n}}{R}\widehat{\phi}\quad(139)$$

If $\beta=0$, it is straightforward to demonstrate that $\widetilde{\mathbf{k}}=\mathbf{k}$. In addition, the relation $\widetilde{\mathbf{k}}\cdot\mathbf{b}=\mathbf{k}\cdot\mathbf{b}$ or

$$\sigma_I b_P\frac{\widetilde{m}}{r}\cos\alpha+\sigma_B b_T\frac{\widetilde{n}}{R}=\sigma_I b_P\frac{m}{r}\cos\alpha+\sigma_B b_T\frac{n}{R}\quad(140)$$

is also well satisfied whatever β, as expected from the initial assumption on the invariance of $k_\parallel$ with the rotation of angle β, which is intrinsically considered in the Rodrigues formula (137).

In the cold limit approximation, the plasma has bi-refringent optical properties which means that for a given $k_\parallel$, the dispersion relation cannot have more than two different roots in $k_\perp$.

From the definitions $\mathbf{k}_\perp=\mathbf{k}\times\mathbf{b}$ and $\mathbf{k}'_\perp=\mathbf{k}'\times\mathbf{b}$, the relation $\mathbf{k}_\perp\cdot\mathbf{k}'_\perp=k_\perp k'_\perp\cos\beta$ becomes

$$(\mathbf{k}\times\mathbf{b})\cdot(\mathbf{k}'\times\mathbf{b})=(\mathbf{k}\cdot\mathbf{k}')\,(\mathbf{b}\cdot\mathbf{b})-(\mathbf{k}\cdot\mathbf{b})\,(\mathbf{b}\cdot\mathbf{k}')=\mathbf{k}\cdot\mathbf{k}'-k_\parallel^2$$

and

$$k_\perp k'_\perp \cos\beta = k_\rho k'_\rho \left\|\nabla\rho\right\|^2 + \frac{mm'}{r^2} + \frac{nn'}{R^2} - \frac{\left\|\nabla\rho\right\|\sin\alpha}{r}\left(mk'_\rho + m'k_\rho\right) - k_\parallel^2 \tag{141}$$

For like mode scattering, $k'_\perp = k_\perp$ and

$$k_\perp^2 \cos\beta = k_\rho k'_\rho \left\|\nabla\rho\right\|^2 + \frac{mm'}{r^2} + \frac{nn'}{R^2} - \frac{\left\|\nabla\rho\right\|\sin\alpha}{r}\left(mk'_\rho + m'k_\rho\right) - k_\parallel^2 \tag{142}$$

a relation which can be well verified by replacing $\left(k'_\rho \left\|\nabla\rho\right\|, \frac{m'}{r}, \frac{n'}{R}\right)$ from (138) into (142). Therefore, for like mode scattering, $\left(k'_\rho, m', n'\right)$ have just to be deduced from (138) knowing (k_ρ, m, n).

For unlike mode scattering, $k'_\perp \neq k_\perp$,

Therefore, The coordinates of $\mathbf{k}'$ are therefore determined by relations (**??**) and (136) and (128),

$$k'_\rho = \frac{1}{\left\|\nabla\rho\right\|}\left[\sin\alpha\frac{m'}{r} + \sigma_\rho\sqrt{k_\parallel^2 + k_\perp'^2 - \cos^2\alpha\frac{m'^2}{r^2} - \frac{n'^2}{R^2}}\right] \tag{143}$$

By definition, the variation of the poloidal mode number m is made possible by the breaking of the toroidal symmetry resulting from the fluctuations, so that the toroidal mode number n is no more conserved in the scattering process.

B.5 Calculation of $\left\|\nabla\rho\right\|$

So far the only restriction over the radial coordinate ρ is that it is a monotonic flux function going from 0 at the center to 1 at the edge. In the code we take $\rho\left(\psi\right) = r\left(\psi, 0\right)/a_p$ where r is defined as a function of (ψ, θ) and $a_p = r\left(\psi_a, 0\right)$. Using

$$\nabla\rho = \frac{d\rho}{d\psi}\left\|\nabla\psi\right\|\hat{\psi} \tag{144}$$

we find

$$\boxed{\left\|\nabla\rho\right\| = \left.\frac{\partial r}{\partial\psi}\right|_{\theta=0}\frac{RB_P}{a_p}} \tag{145}$$

C Susceptibility tensor and dispersion relation

C.1 Cold plasma model

In the cold plasma model $\mathbb{X}^{s\mathrm{C}}$ is independent of $\mathbf{N}$. Also, $X^{s\mathrm{C}}_{xz} = X^{s\mathrm{C}}_{yz} = 0$ and $X^{s\mathrm{C}}_{xx} = X^{s\mathrm{C}}_{yy}$.

$$\begin{aligned} X^{s\mathrm{C}}_\perp &\equiv X^{s\mathrm{C}}_{xx} = X^{s\mathrm{C}}_{yy} = -\frac{\overline{\omega}^2_{ps}}{1-\overline{\omega}^2_{cs}} \\ X^{s\mathrm{C}}_\parallel &\equiv X^{s\mathrm{C}}_{zz} = -\overline{\omega}^2_{ps} \\ X^{s\mathrm{C}}_\times &\equiv iX^{s\mathrm{C}}_{xy} = \frac{\overline{\omega}^2_{ps}\overline{\omega}_{cs}}{1-\overline{\omega}^2_{cs}} \end{aligned} \tag{146}$$

Therefore, $P^{\mathrm{C}}_3 = P^{\mathrm{C}}_1 = 0$ so that

$$\mathcal{D}^{\mathrm{C}}\left(\mathbf{k}, \omega\right) = P^{\mathrm{C}}_4 N^4_\perp + P^{\mathrm{C}}_2 N^2_\perp + P^{\mathrm{C}}_0$$

with

$$\begin{aligned} P_4^{\mathrm{C}} &= K_\perp^{\mathrm{C}} \\ P_2^{\mathrm{C}} &= \left(N_\parallel^2 - K_\perp^{\mathrm{C}}\right)\left(K_\perp^{\mathrm{C}} + K_\parallel^{\mathrm{C}}\right) + \left(K_\times^{\mathrm{C}}\right)^2 \\ P_0^{\mathrm{C}} &= K_\parallel^{\mathrm{C}}\left[\left(N_\parallel^2 - K_\perp^{\mathrm{C}}\right)^2 - \left(K_\times^{\mathrm{C}}\right)^2\right] \end{aligned} \tag{147}$$

where $K_\perp^{\mathrm{C}} = 1 + \sum_s X_\perp^{s\mathrm{C}}$, $K_\parallel^{\mathrm{C}} = 1 + \sum_s X_\parallel^{s\mathrm{C}}$, $K_\times^{\mathrm{C}} = \sum_s X_\times^{s\mathrm{C}}$.

D Kinetic plasma model

The kinetic plasma susceptibility tensor $\mathbb{X}_{\mathrm{M}}$ for a non-relativistic is the sum over contributions from all species

$$\mathbb{X}_{\mathrm{M}} = \sum_s \mathbb{X}_{\mathrm{M}}^s \tag{148}$$

$\mathbb{X}_{\mathrm{M}}^s$ being itself the sum over contributions from all harmonics numbers n

$$\mathbb{X}_{\mathrm{M}}^s = \overline{\omega}_{ps}^2 \zeta_{0s} \sum_{n=-\infty}^{n=+\infty} \mathbb{Y}_{\mathrm{M}}^{s,n} \tag{149}$$

where

$$\begin{aligned} Y_{\mathrm{M},xx}^{s,n} &= \frac{n^2}{\lambda_s}\Gamma_{ns} Z_{ns} \\ Y_{\mathrm{M},yy}^{s,n} &= \left(\frac{n^2}{\lambda_s}\Gamma_{ns} - 2\lambda_s n^2 \Gamma'_{ns}\right) Z_{ns} \\ Y_{\mathrm{M},zz}^{s,n} &= -\Gamma_{ns}\zeta_{ns} Z'_{ns} \\ Y_{\mathrm{M},xy}^{s,n} &= i\sigma_s n \Gamma'_{ns} Z_{ns} \\ Y_{\mathrm{M},yx}^{s,n} &= -Y_{\mathrm{M},xy}^{s,n} \\ Y_{\mathrm{M},xz}^{s,n} &= -\sigma_\parallel \frac{n}{\sqrt{2\lambda_s}}\Gamma_{ns} Z'_{ns} \\ Y_{\mathrm{M},xz}^{s,n} &= Y_{\mathrm{M},zx}^{s,n} \\ Y_{\mathrm{M},yz}^{s,n} &= i\sigma_s\sigma_\parallel \sqrt{\frac{\lambda_s}{2}}\Gamma'_{ns} Z'_{ns} \\ Y_{\mathrm{M},zy}^{s,n} &= -Y_{\mathrm{M},yz}^{s,n} \end{aligned} \tag{150}$$

with

$$\begin{aligned} \Gamma_{ns} &= e^{-\lambda_s} I_n(\lambda_s) \\ Z_{ns} &= Z(\zeta_{ns}) \\ \lambda_s &= \left(N_\perp \overline{\omega}_{cs} \beta_{Ts}\right)^2 \\ \zeta_{ns} &= \frac{1 - n\overline{\omega}_{cs}}{\sqrt{2}\left|N_\parallel\right|\beta_{Ts}} \\ \sigma_s &= \mathrm{sign}(q_s) \\ \sigma_\parallel &= \mathrm{sign}\left(N_\parallel\right) \end{aligned}$$

where $I_n\left(N_\parallel\right)$ is the modified Bessel function of the first kind and $Z\left(N_\parallel\right)$ is the plasma dispersion function [13].

E Benchmarking of C3PO

E.1 JET-like plasma

E.1.1 Equilibrium

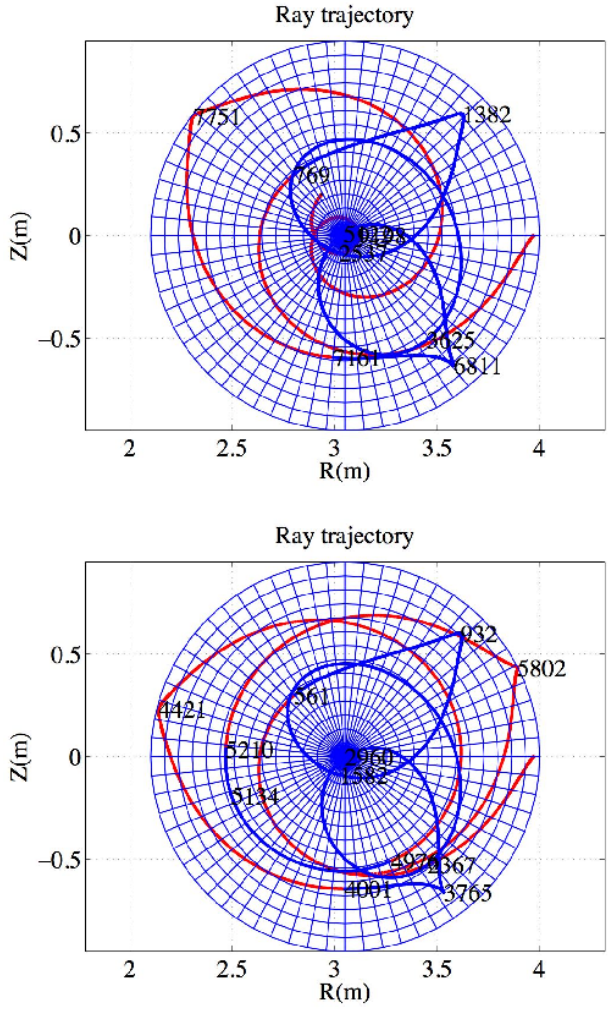

Figure 1: Poloidal projection of the ray trajectory. The red curve corresponds to the slow mode and the blue curve corresponds to the fast mode. Numeric (upper plot) and analytic (lower plot) magnetic equilibrium. $N_{\phi 0} = -2.0$

A JET-like equilibrium was used in Ref.[16] where results from a ray-tracing code using the cold plasma model is presented. A circular concentric toroidal plasma is considered such that

$$\rho = \frac{r}{a_p} \tag{151}$$

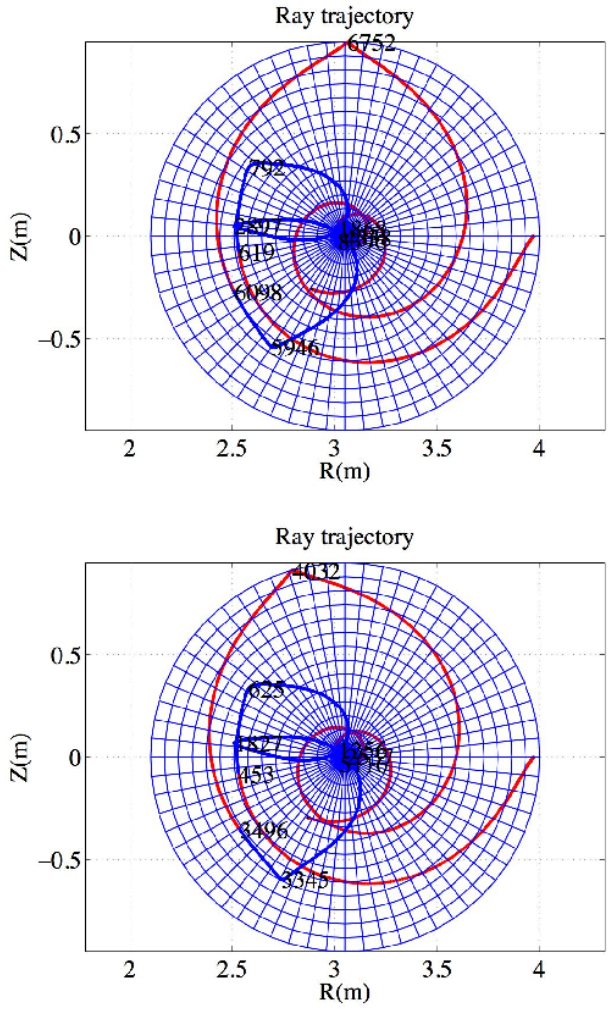

Figure 2: Poloidal projection of the ray trajectory. The red curve corresponds to the slow mode and the blue curve corresponds to the fast mode. Numeric (upper plot) and analytic (lower plot) magnetic equilibrium. $N_{\phi 0} = -1.8$

with the following equilibrium parameters

R_p	3.05 m
a_p	0.95 m
$\hat{B}_T$	3.2 T
I_p	3.5 MA

(152)

and the following profiles

$$\begin{aligned} n_e(\rho) &= (n_{e0} - n_{ea})(1-\rho^2) + n_{ea} \\ J_z(\rho) &= J_0 (1-\rho^2)^{\alpha} \end{aligned} \tag{153}$$

with

$$\begin{aligned} n_{e0} &= 5 \times 10^{19}\ \mathrm{m}^{-3} \\ n_{ea} &= 0.01 \times 10^{19}\ \mathrm{m}^{-3} \end{aligned} \tag{154}$$

The total current is then

$$I_P = 2\pi \int_0^{a_p} J_z r dr = \pi J_0 \frac{a_p^2}{(\alpha+1)} \tag{155}$$

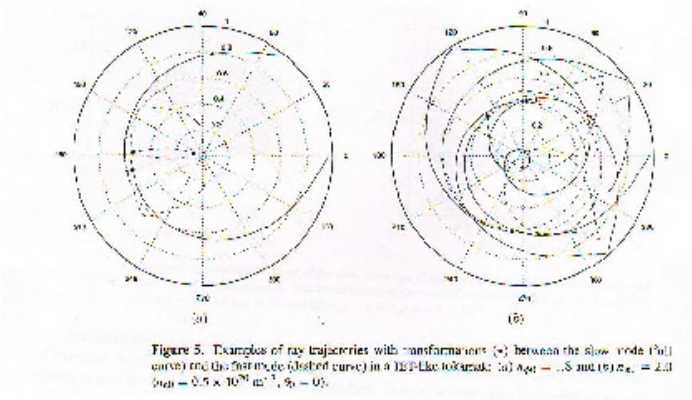

Figure 3: Poloidal projection of the ray trajectory from Ref.[16]

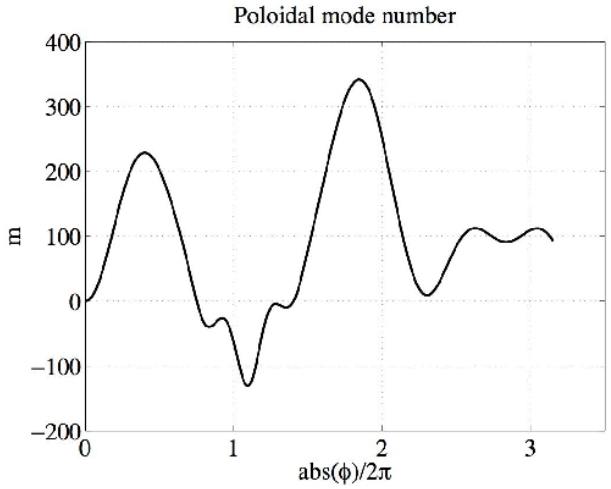

Figure 4: Poloidal mode number along the ray trajectory. (Numeric magnetic equilibrium). $N_{\phi 0} = -2.0$.

such that

$$J_0 = \frac{(\alpha+1)\, I_P}{\pi a_p^2} \tag{156}$$

The magnetic field profile is

$$\begin{aligned} B_T &= \hat{B}_T \frac{R_p}{R} \\ B_P &= \hat{B}_P \frac{R_p}{R} \end{aligned} \tag{157}$$

Ampere's law gives in the small aspect ratio limit (consistent with concentric flux surfaces)

$$\frac{1}{r}\frac{d}{dr}\left(r\hat{B}_P\right) = \mu_0 J_z \tag{158}$$

we get

$$\hat{B}_P = \frac{1}{r}\mu_0 J_0 \int_0^r r\left(1-\frac{r^2}{a_p^2}\right)^{\alpha} dr = \frac{\hat{B}_{Pa}}{\rho}\left[1-\left(1-\rho^2\right)^{\alpha+1}\right] \tag{159}$$

with

$$\hat{B}_{Pa} = \frac{\mu_0 I_P}{2\pi a_p} \tag{160}$$

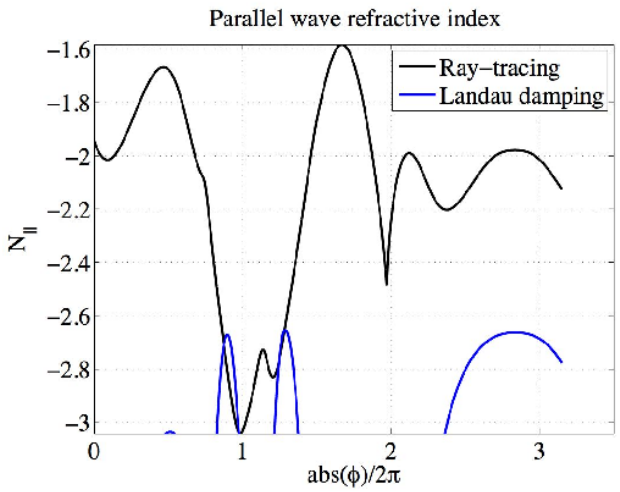

Figure 5: Parallel refractive index or refraction along the ray trajectory. (Numeric magnetic equilibrium). $N_{\phi 0} = -2.0$.

The poloidal flux coordinate $\psi = R_p \int_0^r B_P dr$ is then

$$\psi = R_p \frac{\mu_0 I_P}{2\pi} \int_0^\rho \frac{1}{\rho} \left[1 - \left(1-\rho^2\right)^{\alpha+1}\right] d\rho \tag{161}$$

In the case $\alpha = 1$ it gives

$$\psi = R_p \frac{\mu_0 I_P}{2\pi} \int_0^\rho \frac{1}{\rho} \left[1 - \left(1-\rho^2\right)^{2}\right] d\rho \tag{162}$$

Defining $\rho = \sin\theta$

$$1 - \rho^2 = \cos^2\theta$$
$$d\rho = \cos\theta d\theta$$

yields

$$\begin{aligned}\psi &= R_p \frac{\mu_0 I_P}{2\pi} \int_0^\theta \sin\theta \left[1 + \cos^2\theta\right] \cos\theta d\theta \\ &= R_p \frac{\mu_0 I_P}{2\pi} \rho^2 \left[1 - \frac{1}{4}\rho^2\right]\end{aligned} \tag{163}$$

and finally for $\alpha = 1$ we gather

$$\boxed{\begin{aligned} J_z &= \frac{2I_P}{\pi a_p^2}\left(1-\rho^2\right) \\ \hat{B}_P &= \frac{\mu_0 I_P}{2\pi a_p}\frac{1}{\rho}\left[1-\left(1-\rho^2\right)^2\right] \\ \psi &= R_p \frac{\mu_0 I_P}{2\pi}\rho^2\left[1-\frac{1}{4}\rho^2\right] \end{aligned}}$$

Note that the q profile is approximately (to order ϵ)

$$q \simeq \frac{r}{R_p}\frac{B_T}{B_P} \simeq \frac{r}{R}\frac{\hat{B}_T}{B_P} \tag{164}$$

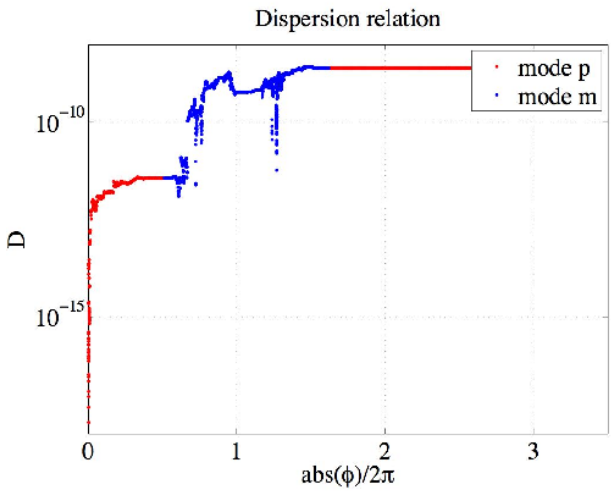

Figure 6: Dispersion relation along the ray trajectory. (Numeric magnetic equilibrium). $N_{\phi 0} = -2.0$.

which gives

$$q \simeq q_{\max} \frac{\rho^2}{1 - (1 - \rho^2)^{\alpha+1}} \tag{165}$$

and for $\alpha = 1$

$$\boxed{q \simeq q_{\max} \frac{\rho^2}{1 - (1 - \rho^2)^2}} \tag{166}$$

where

$$q_{\max} = \frac{\hat{B}_T}{\hat{B}_{Pa}} \frac{a_p}{R_p} \tag{167}$$

Note that $q(0) = q_{\max}/(1+\alpha)$ and $dq/d\rho(0) = 0$.

E.1.2 Wave initial conditions

The ray is launched in the slow mode from the position

$$\begin{aligned} \rho_0 &= 0.968 \\ \theta_0 &= 0 \\ \phi_0 &= 0 \end{aligned} \tag{168}$$

with the spectral properties

$$\begin{aligned} \omega/(2\pi) &= 3.7 \text{ GHz} \\ N_{\phi 0} &= 2.0 \\ m_0 &= 0 \end{aligned} \tag{169}$$

From (131) the initial n can be determined

$$n_0 = \frac{\omega R_0}{c} N_{\phi 0} \tag{170}$$

and then the parallel index of refraction is

$$N_{\|0} = \sigma_B \frac{B_T}{B} N_{\phi 0} \tag{171}$$

E.1.3 Results

The results are plotted in figures 1-6. The wave is mode-converted between the slow to the fast mode several times. The results agree remarkably well with those from Ref.[16]. A small difference in the ray path between the analytical and the interpolated magnetic equilibria is observed in the case $N_{\phi 0} = -1.8$. The deviation is certainly due to the ray passing near the center of the plasma where the numerical interpolation is intrinsically less accurate.

E.1.4 Numerical performances

The magnetic equilibrium is defined on a numerical grid of size (101×65) along the radial and poloidal direction respectively. It is vectorized using a Fourier series expansion with 32 harmonics and the Matlab built-in cubic spline interpolation for the Fourier coefficients. The vectorization procedure takes typically 8.3 seconds on computer equipped with a 64 bits biprocessor AMD opteron clocked at 2.4 GHz, with 4 GBytes of RAM memory.

Ray calculation parameters for the example presented here are typical of tokamak current drive simulation. Ray parameters are stored in the memory each time the radial increment $\Delta\rho$ is larger than 10^{-4}. $\Delta\rho$ may be adapted depending upon the problem. In the 6^{th} order Runge-Kutta procedure, the generalized incremental step h is adjusted so that the norm[6] of the variation along the six directions of extrapolation never exceeds the tolerance level which is set to 10^{-12}. The tolerance level is arbitrarily chosen so that the ray trajectory as well as all wave parameters are independent of its value. Below 10^{-12}, the gain on the ray accuracy is marginal while the computer time increases.

The initial time increment is set to $h_0 = 10^{-4}$ in normalized units, and the calculation ends when $t_{\text{end}} = 10000$, with a maximum of 60000 values stored in the memory. Since the time step h evolves along the ray trajectory depending upon the ray curvature, the effective number of steps is typically much less that t_{end}/h_0. For the current example t_{end} is reached after 5499 steps.

Using the numerical equilibrium, the ray trajectory is calculated in 35.15 seconds, while it takes only 1.21 seconds with the analytic equilibrium. Although the numerical equilibrium is more time consuming by at least an order of magnitude, typical calculation times remain at an acceptable low level for realistic time-dependent tokamak simulations, which require several hundred ray trajectories calculations.

E.2 VERSATOR II and PLT plasmas

E.2.1 Equilibrium

Lower Hybrid heating and current drive simulations have been performed for the VERSATOR II and PLT tokamaks, which both have almost circular concentric magnetic flux surfaces [1, 10]. For the sake of benchmarking, the Shafranov shift is neglected, and a

[6]The infinite norm $\|\mathbf{X}\|_\infty = \max_{i\in[1,N]}(|X_i|)$ is used, where N is the dimension of the vector $\mathbf{X}$.

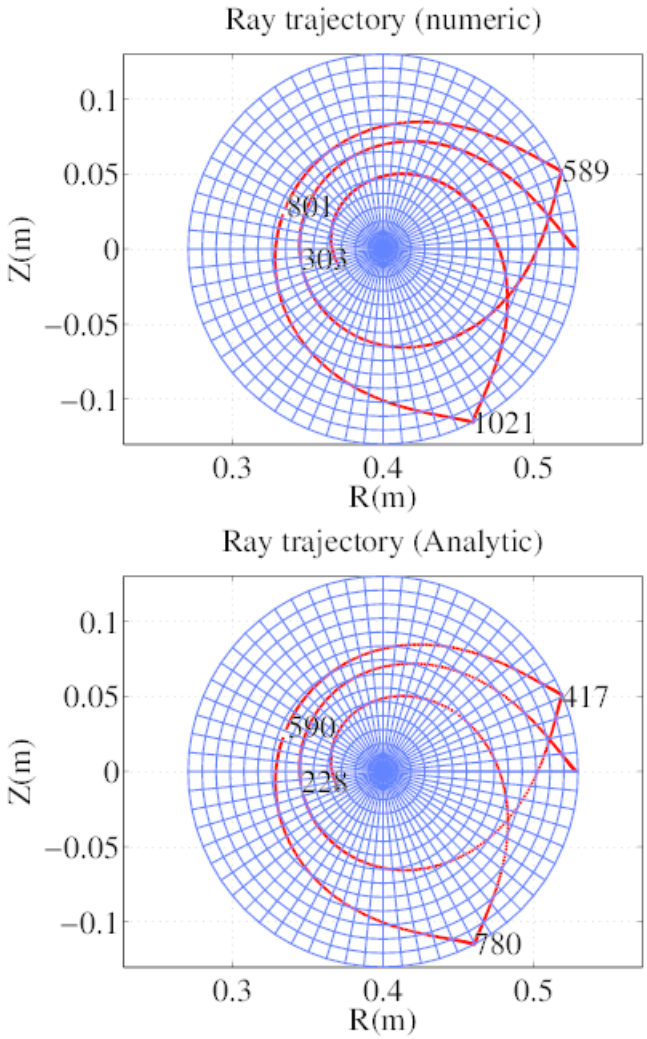

Figure 7: Poloidal projection of the ray trajectory. The red curve corresponds to the slow mode and the blue curve corresponds to the fast mode. Numeric (upper plot) and analytic (lower plot) magnetic equilibrium. VERSATOR II. $N_{\|0} = 5.0$.

plasma with exact circular concentric magnetic flux surfaces is considered with the following magnetic equilibrium parameters

	VERSATOR II	PLT
R_p	0.4 m	1.32 m
a_p	0.13 m	0.4 m
$\hat{B}_T$	1.4 T	3.1 T
I_p	0.05 MA	0.2 MA

(172)

and the following profiles

$$n_e\left(\rho\right) = \left(n_{e0} - n_{ea}\right) \frac{e^{\alpha_n} - e^{\alpha_n \rho^2}}{e^{\alpha_n} - 1} + n_{ea} \tag{173}$$

with

	VERSATOR II	PLT
n_{e0}	2.0×10^{19} m^{-3}	0.5625×10^{19} m^{-3}
n_{ea}	2.0×10^{18} m^{-3}	0.5625×10^{18} m^{-3}
α_n	0.1	−0.571

(174)

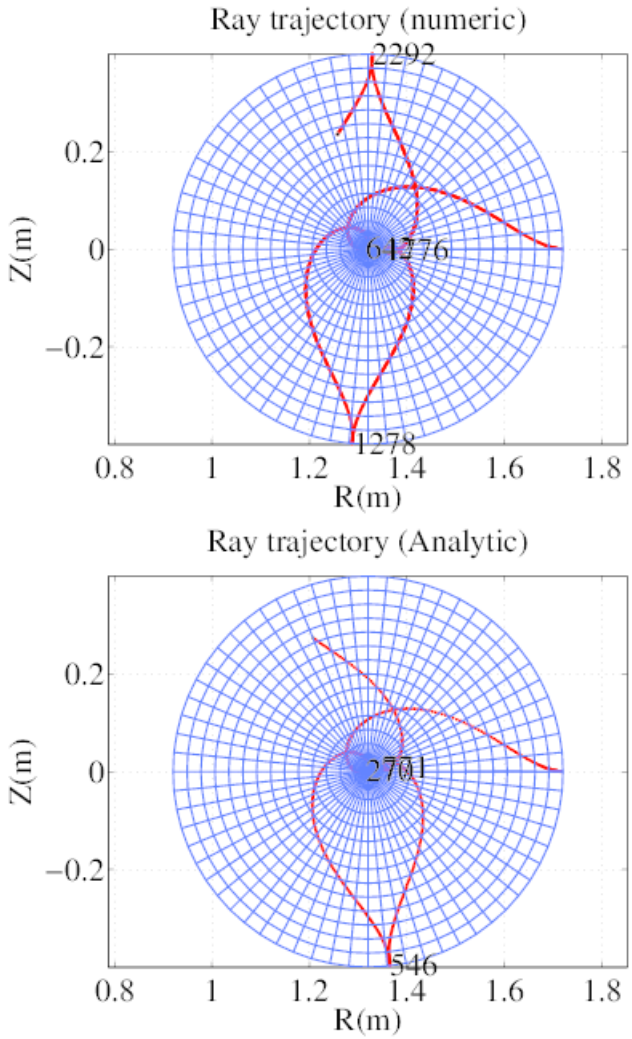

Figure 8: Poloidal projection of the ray trajectory. The red curve corresponds to the slow mode and the blue curve corresponds to the fast mode. Numeric (upper plot) and analytic (lower plot) magnetic equilibrium. PLT, $N_{\|0} = 1.33$.

In the calculations, the scrape-off layer is not considered, since the specular reflection is enforced if needed on the last closed magnetic surface for the Lower Hybrid wave.

For both tokamaks, Z_{eff} is uniform with $Z_{\text{eff}} = 4$ for VERSATOR II and $Z_{\text{eff}} = 2$ for PLT. The plasma is made of hydrogen ions for VERSATOR II and deuterium ions for PLT. For both machines, a fully stripped single impurity species is considered, using carbon ions with $m_c = 12$, $Z_c = 6$.

The magnetic equilibrium is characterized by a parabolic safety factor profile

$$q(\rho) = q_{\min} + (q_{\max} - q_{\min})\,\rho^2 \tag{175}$$

The poloidal flux coordinate ψ is then

$$\psi = \frac{1}{2}\frac{\hat{B}_T a_p^2}{q_{\max} - q_{\min}} \ln\left[\frac{q(\rho)}{q_{\min}}\right] \tag{176}$$

which leads to

$$\psi_a = \frac{1}{2}\frac{\hat{B}_T a_p^2}{q_{\max} - q_{\min}} \ln\left[\frac{q_{\max}}{q_{\min}}\right] \tag{177}$$

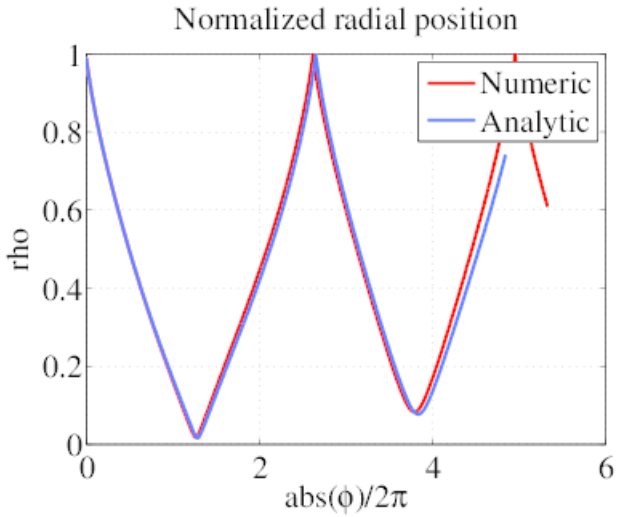

Figure 9: Radial position of the ray trajectory as function of the toroidal angle (PLT). $N_{\|} = 1.33$.

In the simulations, $q_{\min} = 1$, and $q_{\max}$ is obtained from Ampère's law.

E.2.2 Wave initial conditions

For both tokamaks, the ray is launched in the slow mode from the position

$$\begin{aligned} \rho_0 &= 0.99 \\ \theta_0 &= 0 \\ \phi_0 &= 0 \end{aligned} \tag{178}$$

with the spectral properties

	VERSATOR II	PLT
$\omega/(2\pi)$	0.8 GHz	0.8 GHz
$N_{\|0}$	5.0	1.33
m_0	-25	$+20$

(179)

The non-zero m_0 arises from the fact that simulations in references [1] [10] use $m_0 = 0$ in the scrape-off layer and not at $\psi = \psi_a$.

E.2.3 Results

The results are plotted in figures 7-12. A good agreement is found with references [1] and [10] despite differences in the magnetic equilibrium. An excellent agreement is found between numerical and analytical magnetic equilibrium for the case of VERSATOR II where the ray never approaches the plasma center.

The difference arises from a cumulative error that becomes more important when the ray approaches the plasma center. Yet the effect on the wave power and current deposition generally remains negligible.

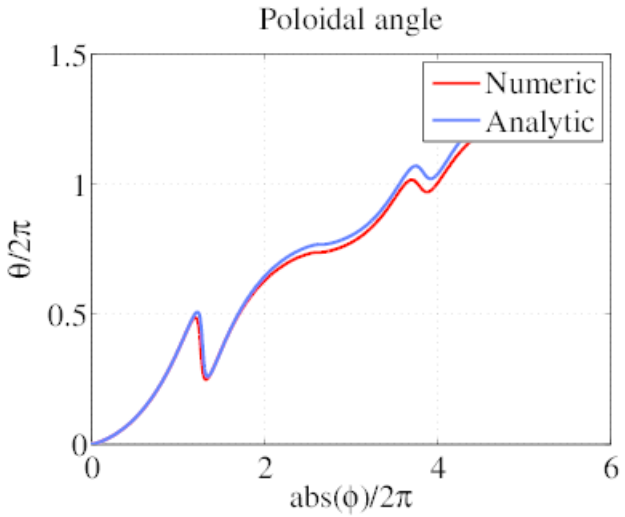

Figure 10: Poloidal position of the ray trajectory as function of the toroidal angle (PLT). $N_{\|} = 1.33$.

E.3 Propagation in toroidal vacuum device

E.3.1 Magnetic configuration

In vacuum, electromagnetic waves trajectories are straight lines, which offers an interesting benchmarking case for the curvilinear coordinate system used with $C3PO$ ray-tracing. It is enforced that at $\psi = \psi_a$ the wave is reflected like in a mirror, so that the ray remains confined in the machine. Circular concentric poloidal magnetic flux surfaces are considered with

R_p	3.0 m
a_p	0.9 m
$\hat{B}_T$	3.0 T

(180)

and the poloidal magnetic field is considered to be created by a virtual toroidal current I_p of 1.0 MA and a parabolic safety factor profile of the form

$$q(\rho) = q_{\min} + (q_{\max} - q_{\min})\,\rho^2 \tag{181}$$

with $q_{\min} = 1$ and $q_{\max}$ obtained from Ampère's law.

Since rays are straight lines, it is possible to calculate the exact rays trajectories from geometrical arguments. Since $\|\nabla\rho\| = 1$, the initial value of the wave vector is $\mathbf{k}_0 = k_{\rho 0}\widehat{\rho} + k_{\theta 0}\widehat{\theta} + k_{\phi 0}\widehat{\phi}$ with $k_{\theta 0} = m_0 a_p/\rho_0$ and $k_\phi = n_0 a_p/R_0$. $\mathbf{k}_0$ is expressed in cartesian coordinates using the relation $\mathbf{k}_0^{cartesian} = \mathbb{M}_{cc}(\theta_0, \phi_0) \cdot \mathbf{k}_0^{curvilinear}$ where

$$\mathbb{M}_{cc}(\theta, \phi) = \begin{pmatrix} \cos\theta\cos\phi & -\sin\theta\cos\phi & -\sin\phi \\ \cos\theta\sin\phi & -\sin\theta\sin\phi & \cos\phi \\ \sin\theta & \cos\theta & 0 \end{pmatrix} \tag{182}$$

The initial position at launch in the cartesian coordinates $(\overline{x}_0, \overline{y}_0, \overline{z}_0)$ normalized to a_p is

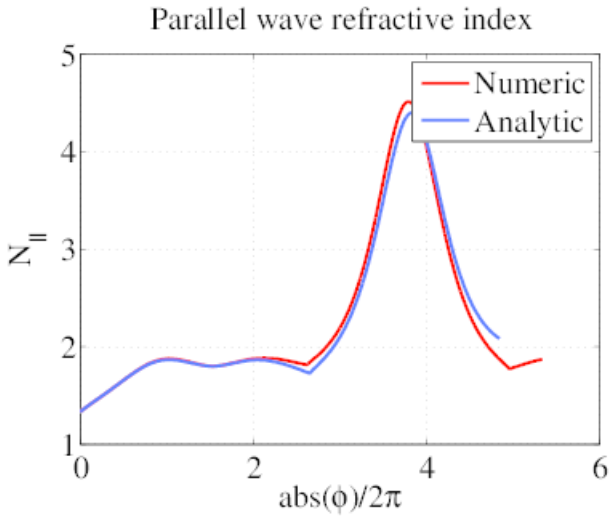

Figure 11: Parallel refractive index or refraction along the ray trajectory as function of the toroidal angle (PLT). $N_{\|} = 1.33$.

given by the relations

$$\begin{aligned} \overline{x}_0 &= \left(\frac{R_p}{a_p} + \rho_0 \cos\theta_0\right) \cos\phi_0 \\ \overline{y}_0 &= \left(\frac{R_p}{a_p} + \rho_0 \cos\theta_0\right) \sin\phi_0 \\ \overline{z}_0 &= \rho_0 \sin\theta_0 \end{aligned} \tag{183}$$

where $(\rho_0, \theta_0, \phi_0)$ are initial curvilinear coordinates. Since the ray is a straight line, its position is given by the parametric equation

$$\begin{aligned} \overline{x}^{(l)} &= \overline{x}_0 + k_{x0} s\,(l)\,/k_0 \\ \overline{y}^{(l)} &= \overline{y}_0 + k_{y0} s\,(l)\,/k_0 \\ \overline{z}^{(l)} &= \overline{z}_0 + k_{z0} s\,(l)\,/k_0 \end{aligned} \tag{184}$$

where $s\,(l)$ is the ray length starting from $s\,(l=0) = 0$ at $(\overline{x}_0, \overline{y}_0, \overline{z}_0)$ .Once $\left(\overline{x}^{(l)}, \overline{y}^{(l)}, \overline{z}^{(l)}\right)$ known, it is possible to determine back (ρ, θ, ϕ) by inverting (183). From the determination of (ρ, θ, ϕ) , it is possible to evaluate $\mathbf{k}_l^{curvilinear}$at all positions, using $\mathbf{k}_l^{cartesian} = \mathbf{k}_0^{cartesian}$ and

$$\mathbf{k}_l^{curvilinear} = \mathbb{M}_{cc}^{-1}\,(\theta, \phi) \cdot \mathbf{k}_0^{cartesian} \tag{185}$$

Then $m^{(l)} = k_\theta^{(l)} \rho^{(l)}/a_p$ and $n^{(l)} = k_\phi^{(l)} R^{(l)}/a_p$

In order to keep the ray inside the toroidal chamber, a specular reflection is enforced at ψ_a.If the condition $\rho^{(l)} > 1$ is encountered, then the new direction of the ray $\mathbf{k}_{0(i+1)}^{cartesian}$ of the $i+1$ ray segment is deduced from $\mathbf{k}_{0(i)}^{cartesian}$ according to the conditions

$$\mathbf{k}_{0(i+1)}^{cartesian} \cdot \widehat{\rho}^{(l-1)} = -\mathbf{k}_{0(i)}^{cartesian} \cdot \widehat{\rho}^{(l-1)} \tag{186}$$

$$\mathbf{k}_{0(i+1)}^{cartesian} \cdot \widehat{\theta}^{(l-1)} = \mathbf{k}_{0(i)}^{cartesian} \cdot \widehat{\theta}^{(l-1)} \tag{187}$$

$$\mathbf{k}_{0(i+1)}^{cartesian} \cdot \widehat{\phi}^{(l-1)} = \mathbf{k}_{0(i)}^{cartesian} \cdot \widehat{\phi}^{(l-1)} \tag{188}$$

where $\left(\widehat{\rho}, \widehat{\theta}, \widehat{\phi}\right)$ are used at the increment $(l-1)$. It corresponds to the relation

$$\mathbf{k}_{0(i+1)}^{cartesian} = \left[\mathbb{M}_{cc1}^{-1}\left(\theta^{(l-1)}, \phi^{(l-1)}\right) \cdot \mathbb{M}_{cc2}\left(\theta^{(l-1)}, \phi^{(l-1)}\right)\right] \cdot \mathbf{k}_{0(i)}^{cartesian} \tag{189}$$

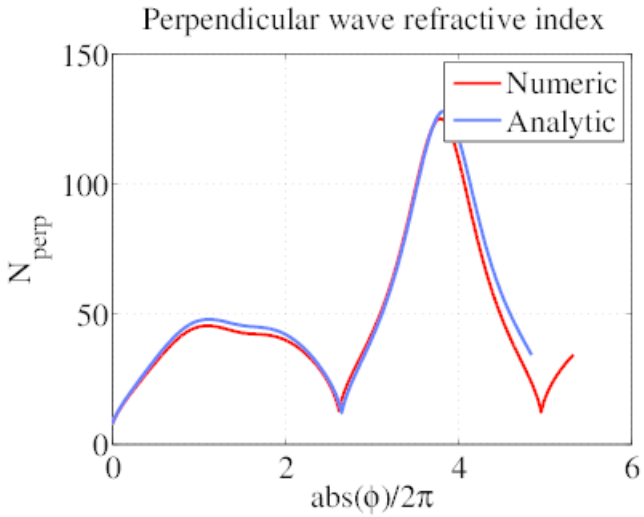

Figure 12: Perpendicular refractive index or refraction along the ray trajectory as function of the toroidal angle (PLT). $N_{\|} = 1.33$.

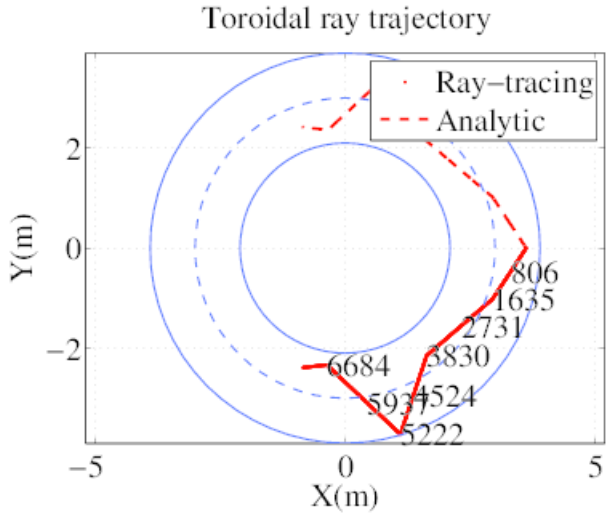

Figure 13: Toroidal projection of the ray trajectory of an electromagnetic wave in vacuum.

with

$$\mathbb{M}_{cc1}(\theta,\phi) = \begin{pmatrix} \cos\theta\cos\phi & \cos\theta\sin\phi & \sin\theta \\ -\sin\theta\cos\phi & -\sin\theta\sin\phi & \cos\theta \\ \sin\phi & -\cos\phi & 0 \end{pmatrix} \tag{190}$$

and

$$\mathbb{M}_{cc2}(\theta,\phi) = \begin{pmatrix} -\cos\theta\cos\phi & -\cos\theta\sin\phi & -\sin\theta \\ -\sin\theta\cos\phi & -\sin\theta\sin\phi & \cos\theta \\ \sin\phi & -\cos\phi & 0 \end{pmatrix} \tag{191}$$

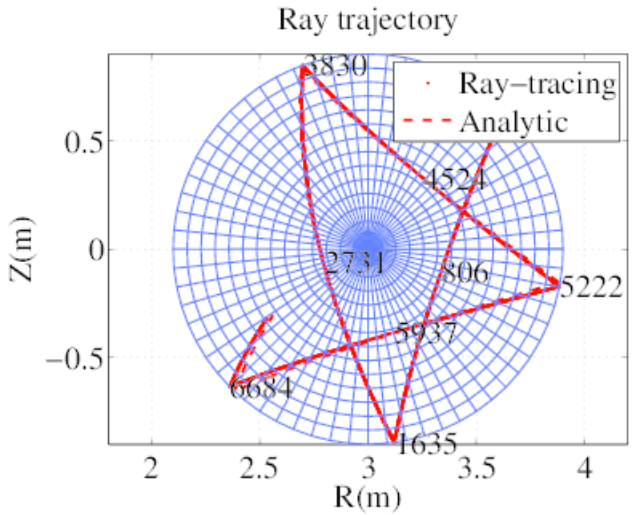

Figure 14: Poloidal projection of the ray trajectory of an electromagnetic wave in vacuum.

E.3.2 Wave initial conditions

In the example here given, the ray is launched from the position

$$\begin{aligned} \rho_0 &= 0.98 \\ \theta_0 &= \pi/4 \\ \phi_0 &= 0 \end{aligned} \tag{192}$$

with spectral properties

$\omega/(2\pi)$	530.15 GHz
$N_{\|\|0}$	0.5
m_0	−3000

(193)

so that the wave can propagate into vacuum region.

E.3.3 Results

As expected, ray trajectory is made of pieces of straight lines, which can be easily shown from the toroidal projection in Fig 13. Because of the toroidal topology, the poloidal projection in Fig. 14 does not give straight lines. This result highlights the fact that it is very difficult to have a correct picture of the ray path from this type of representation. Comparison with simple geometrical optics is excellent.

E.4 Reverse field pinch plasma

E.4.1 Equilibrium

In Reverse Field Pinch, the plasma evolves to a quasi-stationary magnetic equilibrium close to the force free minimum energy states described by Taylor [17]. The fully relaxed Taylor states are characterized by

$$\nabla \times \mathbf{B} = \lambda \mathbf{B} \tag{194}$$

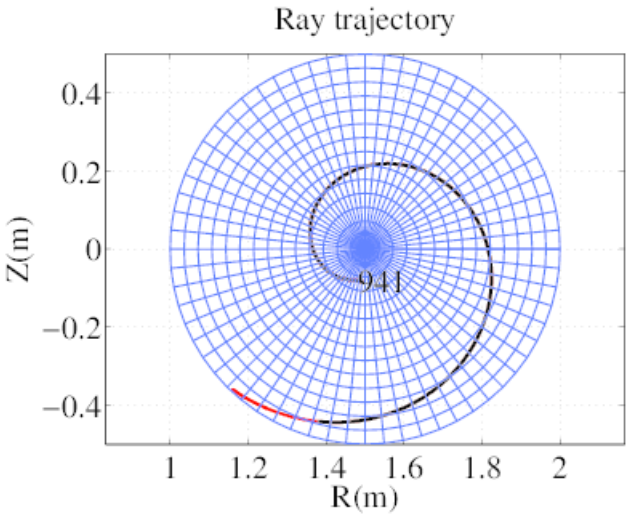

Figure 15: Poloidal projection of the ray trajectory in the slow mode (RFP).

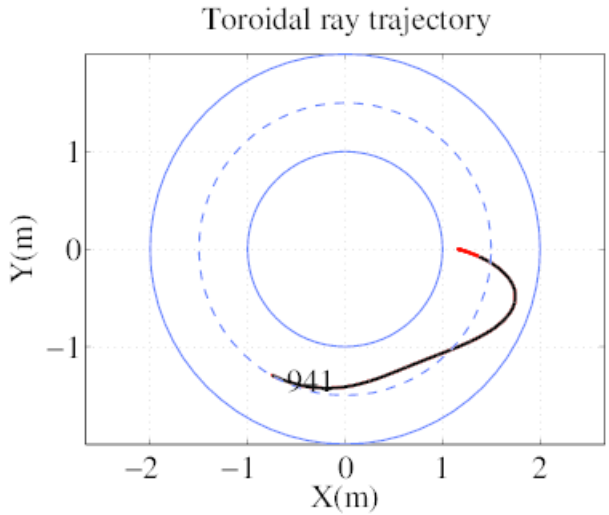

Figure 16: Toroidal projection of the ray trajectory in the slow mode (RFP).

with

$$\lambda = \mu \mathbf{J} \cdot \mathbf{B} / B^2 \tag{195}$$

constant throughout the plasma. A usual simplified approach is to consider a circular concentric toroidal plasma such that

$$\rho = \frac{r}{a_p} \tag{196}$$

with the following equilibrium parameters[7]

R_p	1.5 m
a_p	0.5 m
$\hat{B_T}$	0.2 T
I_p	0.3 MA

(197)

[7]Parameters are corresponding to the large RFP machine of Madison University (USA)

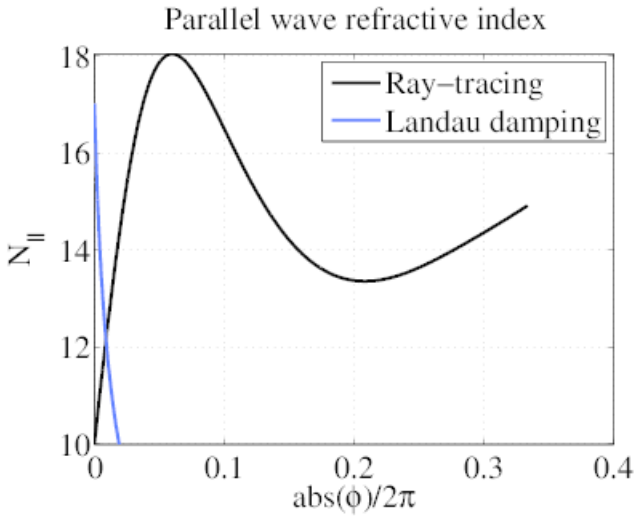

Figure 17: Parallel refractive index or refraction along the ray trajectory (RFP).

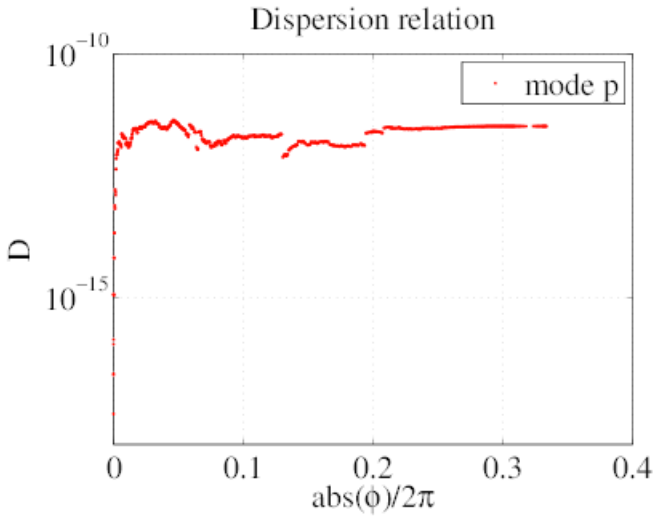

Figure 18: Dispersion relation along the ray trajectory (RFP).

From Eq. 194, considering a constant λ value,

$$(\nabla \times \mathbf{B})_r = \frac{1}{rR}\frac{\partial}{\partial\theta}(RB_\phi) - \frac{1}{R}\frac{\partial}{\partial\phi}(RB_\theta) \tag{198}$$

$$(\nabla \times \mathbf{B})_\theta = -\frac{1}{R}\frac{\partial}{\partial r}(RB_\phi) \tag{199}$$

$$(\nabla \times \mathbf{B})_\phi = \frac{1}{r}\frac{\partial}{\partial r}(rB_\theta) \tag{200}$$

which leads to two coupled equations

$$-\frac{1}{R}\frac{\partial}{\partial r}(RB_\phi) = \lambda B_\theta \tag{201}$$

$$\frac{1}{r}\frac{\partial}{\partial r}(rB_\theta) = \lambda B_\phi \tag{202}$$

Inserting Eq.201 into Eq.202 in order to eliminate B_θ, one finds the equation for B_ϕ

$$\frac{1}{r}\frac{\partial}{\partial r}\left(\frac{r}{R}\frac{\partial}{\partial r}\left(RB_\phi\right)\right) = -\lambda^2 B_\phi \tag{203}$$

which can be developed as

$$\frac{\partial^2}{\partial r^2}\left(RB_\phi\right) + \frac{R}{r}\frac{\partial}{\partial r}\left(\frac{r}{R}\right)\frac{\partial}{\partial r}\left(RB_\phi\right) + \lambda^2 RB_\phi = 0 \tag{204}$$

Assuming a low inverse aspect ratio limit, and neglecting all terms higher than $(a_p/R_p)^2$,

$$\frac{\partial}{\partial r}\left(\frac{r}{R}\right) \simeq \frac{1}{R} \tag{205}$$

and

$$\frac{\partial^2}{\partial r^2}\left(RB_\phi\right) + \frac{1}{r}\frac{\partial}{\partial r}\left(RB_\phi\right) + \lambda^2 RB_\phi = 0 \tag{206}$$

which is a Bessel equation whose solution is

$$RB_\phi = J_0\left(\lambda r\right) \tag{207}$$

Reporting this equation in Eq.201, and using the derivative identity for Bessel functions of order m,

$$\frac{d}{dx}\left(x^m J_m\left(x\right)\right) = x^m J_{m-1}\left(x\right) \tag{208}$$

one finds

$$RB_\theta = -J_{-1}\left(\lambda r\right) = J_{+1}\left(\lambda r\right) \tag{209}$$

From the determination of B_ϕ and B_θ, it turns finally out that $\left(\nabla \times \mathbf{B}\right)_r = 0$, and therefore Eq.194 is well satisfied.

For the ray-tracing calculations, the magnetic equilibrium is chosen so that $\lambda a_p = \widetilde{\lambda} = 2.2$. From these definition, up to the same order, the safety factor is

$$\boxed{q \simeq \frac{a_p}{R_p}\rho\frac{J_0\left(\widetilde{\lambda}\rho\right)}{J_1\left(\widetilde{\lambda}\rho\right)}} \tag{210}$$

For the cold plasma model, the electron density profile is

$$n_e\left(\rho\right) = \left(n_{e0} - n_{ea}\right)\left(1-\rho^2\right)^{\alpha_{n_e}} + n_{ea} \tag{211}$$

with

$$\begin{aligned} n_{e0} &= 1.4 \times 10^{19}\ \mathrm{m}^{-3} \\ n_{ea} &= 0.24 \times n_{e0} \\ \alpha_{n_e} &= 1.3 \end{aligned} \tag{212}$$

while the main plasma gas is Deuterium. Calculations are performed with a uniform effective charge $Z_{eff} = 2$, using the fully stripped single impurity model, with Carbon.

E.4.2 Wave initial conditions

The ray is launched in the slow mode from the position

$$\begin{aligned} \rho_0 &= 0.968 \\ \theta_0 &= 3\pi/4 \\ \phi_0 &= 0 \end{aligned} \tag{213}$$

with the spectral properties

$$\begin{aligned} \omega/\left(2\pi\right) &= 0.8 \text{ GHz} \\ N_{\|0} &= 10.0 \\ n_0 &= 0 \end{aligned} \tag{214}$$

It is worth noting that since at the plasma edge of a RFP, magnetic field lines are almost in the poloidal direction, the toroidal wave number n_0 must be zero, instead of m_0 usually used for tokamaks, where edge magnetic field lines are almost aligned toroidally. Because of the axisymmetry, n remains equal to zero along the ray propagation. Nevertheless, rays may propagate toroidally.

E.4.3 Results

The results are shown in figures 15-18. A strong poloidal upshift is observed as the LH wave propagates, and as found by previous publications, the ray does a spiral around the magnetic axis. Even if the magnetic equilibrium strongly differs from the usual tokamak one, the dispersion relation is well fulfilled along the ray path.

References

[1] P.T. Bonoli. Linear theory of lower hybrid heating. *IEEE Trans. on Plasma Sci.*, PS-12(2):95–107, 1984.

[2] J. P. Bizarro, Y. Peysson, P.T. Bonoli, J. Carrasco, T. Dudok de Wit, V. Fuchs, G. T. Hoang, X. Litaudon, D. Moreau, C. Pocheau, and I. P. Shkarofsky. On self-consistent ray-tracing and fokker-planck modeling of the hard x-ray emission during lower hybrid current drive in tokamaks. *Phys. Fluids B*, 5(9):3276–3283, 1993.

[3] Y. Peysson, R. Arslanbekov, V. Basiuk, J. Carrasco, X. Litaudon, and J. P. Bizarro. Magnetic ripple and the modeling of the lower-hybrid curent drive in tokamaks. *Phys. Plasmas*, 3(10):3668–3688, 1996.

[4] F. Imbeaux and Y. Peysson. Ray-tracing and fokker–planck modelling of the effect of plasma current on the propagation and absorption of lower hybrid waves. *Plasma Phys. Control. Fusion*, 47(11):2041–2065, 2005.

[5] K. Matsuda. Ray tracing study of the electron cyclotron current drive in diii-d using 60 ghz. *IEEE Transactions on Plasma Science*, 17(1):6–11, 1989.

[6] A. P. Smirnov and R. W. Harvey. Calculations of the current drive in diii-d with the genray ray tracing code. *Bull. Amer. Physical Society*, 40:1837, 1995. 37th Annual Meeting of the Division of Plasma Physics November 6-10, 1995 Louisville, Kentucky abstract 8p35.

[7] A. P. Smirnov and R. W. Harvey. The genray ray tracing code. Technical report, Report CompX-2000-01, Ver. 2, 2003.

[8] G. T. A. Huysmans, J. P. Goedbloed, and W. Kerner. Helena code. In Armin Tenner, editor, *CP90 Europhysics Conference on Computational Physics, Amsterdam, the Netherlands, 10-13 September 1990*, page 371. Word Scientific, Singapore, 1991.

[9] J. Decker and Y. Peysson. DKE: A fast numerical solver for the 3D drift kinetic equation. report EUR-CEA-FC-1736, Euratom-CEA, 2004.

[10] P.T. Bonoli and R.C. Englade. Simulation model for lower hybrid current drive. *Phys. Fluids*, 29(9):2937–2950, 1986.

[11] W. H. Press, S. A. Teukolsky, W. T. Vetterling, and B. P. Flannery. *Numerical Recipes in C*. Cambridge University Press, 2nd edition, 1992.

[12] Joan Decker and Abhay K. Ram. Relativistic description of electron Bernstein waves. *Phys. Plasmas*, 13(11), NOV 2006.

[13] M. Brambilla. *Kinetic Theory of Plasma Waves*. Oxford Science Publications, 1998.

[14] P. T. Bonoli and E. Ott. Toroldal and scattering effects on lower-hybrid wave propagation. *Phys. Fluids*, 25(2):359–375, 1982.

[15] G. Vahala, L. Vahala, and P.T. Bonoli. Effect of magnetic and density fluctuations of the propagation of lower-hybrid waves in tokamaks. *Phys. Fluids B*, 4(12):4033–4045, 1992.

[16] J.A. Heikkinen, T.J.J. Tala, T.J.H. Pattikangas, A.D. Piliya, A.N. Saveliev, and S.J. Karttunen. Role of fast waves in the central deposition of lower hybrid power. *Plasma Phys. Control. Fusion*, 41:1231–1249, 1999.

[17] J. B. Taylor. Relaxation of toroidal plasma and generation of reverse magnetic fields. *Phys. Rev. Lett.*, 33(19):1139–1141, 1974.